博士論文

A mathematical and physical approach to improve traffic

flow by non car–following behavior in highways

（高速道路における車両の非追従挙動による

全体の交通流量の向上に関する数理物理学的アプローチ）

谷口洋平

Contents

Chapter 1

Introduction

1.1 Problem of traffic jam

Jams have frequently occurred in road traffic in many countries. Many people suffer from wasted times because of the jams. In fact, the economic losses caused by traffic jams in Japan were approximately 11 trillion yen in 2005 [1]. In highway traffic, there have frequently occurred large scale of jams around urban areas especially in weekends.

What is the causes of the occurrence of the jams? According to NEXCO, which is a company managing expressways in Japan, over 70 % of the jams occurred in expressways are caused by "*traffic concentration*" [2]. Traffic concentration means the states that too many cars move on a road. It is well known that the traffic concentration is occurred in specific locations and at the time or the days when many cars enter and pass the location. Of the locations of the occurrence of traffic concentration, about 62 % is the uphill or the "*sag*", about 30 % is the junction points such as the entrance of expressways and the junction of two expressways, and about 3 % is the entrance or the exit of tunnels [2]. At these locations, cars are easy to brake unconsciously. Sag is a concaved road composed of a downhill and an uphill. If both of the hills are gradual, drivers on the sag are difficult to recognize the gradient and they decelerate unconsciously by the uphill. At junctions, when a car joins a slow lane (a cruising lane) from the junction, a car on the lane moving behind the car brakes to keep a headway for safety. Otherwise, for the reason such that the car on the lane does not want to brake, the car moves to the fast lane (the overtaking lane). Then another car on the fast lane decelerates as well as the car on the slow lane does. In the case of tunnels, drivers sometimes decelerate because of feeling oppressive and dark in tunnels. They also sometimes brake at the exit of the tunnels because of feeling bright. Therefore, at the time such as a rush hour or in a day such as in weekends,

the traffic concentration occurs due to the decrease of cars' velocity at such locations.

The relationship between traffic concentration and traffic jams has been revealed in the field of the study of traffic flow. Traffic flow belongs to a complex system because each of cars composing of traffic flow moves with its own intention. It has been studied in physics for revealing the mechanism of it and in engineering for solving the traffic jams.

Fundamental studies have developed methods to analyze traffic flow and revealed the mechanisms of traffic jams [3–9]. In these studies of traffic flow, the density and flux of the traffic flow are defined: density is the number of cars on a certain load and it represents the degree of traffic congestion on the load. Flux is the number of cars passing a certain point on a load for a period. Flux also can be represented by the product of the density and the mean velocity of the load for the period. The relationship between traffic concentration and jams can be found from the relationship between density and flux of traffic flow. Figure 1.1 shows the density and flux in a two-dimensional diagram at Thuo expressway in Japan in a day. Such the diagram of the density and flux is called a "*fundamental diagram*" in the field of the study of traffic flow. In this figure, the relationship between the density and the flux clearly changes at the certain value of the density, which is called the "*critical density*". The traffic concentration corresponds to the state that the density is around the critical density.

If density is smaller than the critical density, the flux increases linearly as the density increases. This state is called "*free flow*". In free flow, cars can keep at a high velocity thus the flux is proportional to the density. On the other hand, if density is beyond the critical density, the flux rather decrease as the density increases. This state is called "*congested flow*" and corresponds to the state of traffic jam. A traffic concentration often transfers into a traffic jam by some perturbations on a road such as the velocity fluctuation of cars and the reaction time delay by human. In this case, a car on the road decelerates or stops by the perturbations and the following car also decelerates or stops influenced by the behavior of the car. The chain of this deceleration occurs from cars to cars and propagate like a wave. The wave is called "*shock wave*". Shock wave propagates at the velocity from 10 km/h to 20 km/h from the downstream direction (travel direction of cars) to the upstream direction (opposite direction of the travel direction), and the velocity is commonly observed in many countries.

In the field of traffic flow, researchers have found some universality such as the occurrence of the two phases of free flow and congestion flow and the velocity of shock wave. Due to this universality, it is valuable that we model the essence of the phenomenon of

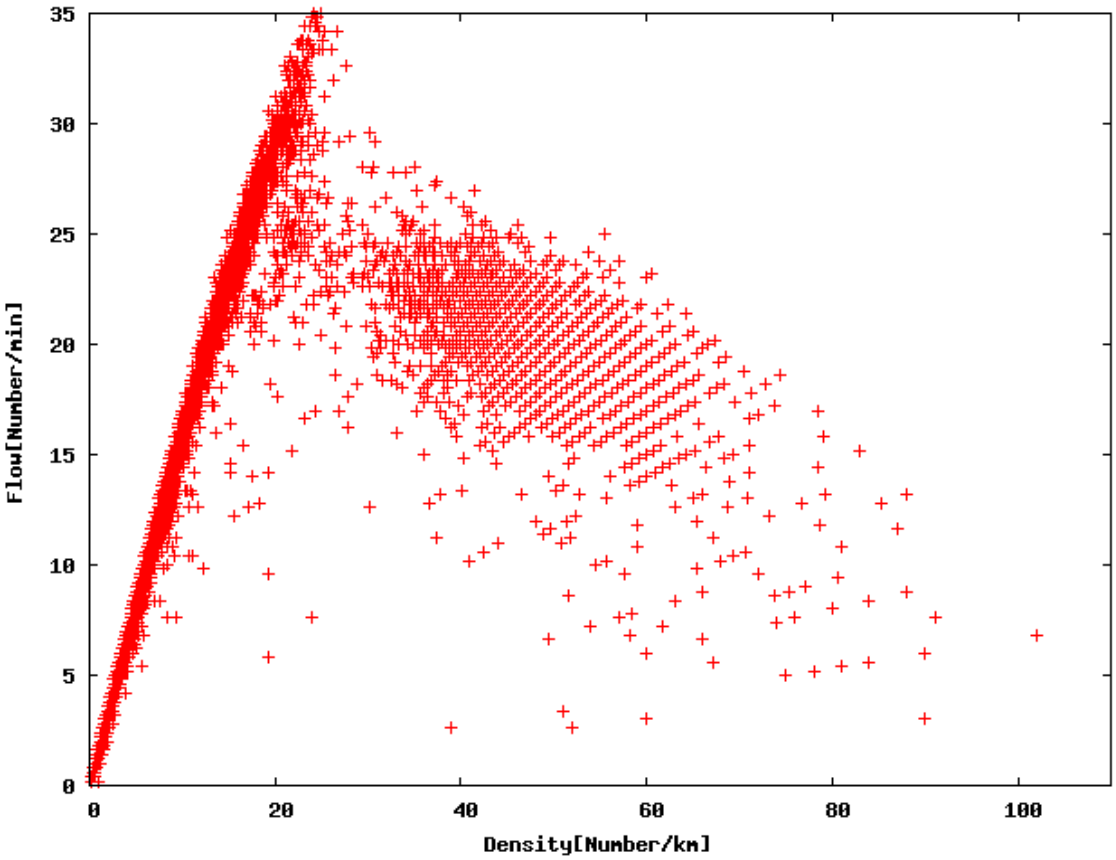

Fig. 1.1. The fundamental diagram of the traffic flow from the empirical data in Thuo expressway.

the traffic flow to understand the phenomenon and to apply for solving the traffic jam.

1.2 Basic research

1.2.1 Mathematical models for the explication of traffic flow

The mechanism of traffic flow has been studied with mathematical models produced in past several decades [4, 5, 9–11]. The models are categorized into "*macroscopic*" and "*microscopic*" model, and are further distinguished whether the variables in the models are continuous or discrete (Tab. 1.1). Macroscopic and microscopic models have progressed separately. Macroscopic models are also called "*fluid model*". In fluid model, traffic is described in macroscopic parameters such as density and flux. On the other hand, in microscopic models, the variables of each car such as the position and velocity are defined. The traffic flow is expressed by the mass of the cars that interact each other. Some of

the microscopic models treat continuous values and the behavior of each car is described in differential equations. These model are called "*car–following model*". In the decade of 1990, the evolution of computation has improved the performance of calculation thus the traffic flow can be observed by numerical simulations with car–following models. Due to this evolution, the study with car–following models has rapidly progressed. At the same time, the study with another type of models which treat discrete parameters also has developed because of the simplicity. In these models, the road is divided into cells and cars move from one cell to another cell. Such models are called "*cellular automaton (CA) model*". We explain details of the fluid, car-following and CA models in the following.

	Model	Time	Space
macroscopic model	fluid model	continuous	continuous
microscopic model	car-following model	continuous	continuous
	cellular automaton model	discrete	discrete

Table. 1.1. The table which describes the characteristics of the three traffic models.

Fluid model

Fluid model is of course based on fluid dynamics and defines the density and flux of traffic flow. It can reproduce the basic characteristic, the relationship between the density and the flow, observed in real traffic. One of the first fluid model was proposed by Lighthill [12] in 1955. It discusses the propagation speed of the shock waves with the knowledge of fluid dynamics. In a model based on Burgers equation, the exact solution of a shock wave behavior in one-dimension fluid has been obtained [13]. Then many researchers have proposed fluid models based on the fluid dynamics [14–18].

Cellular Automaton (CA) model

CA model is simple but can reproduce free flow and congestion flow, which is fundamental property observed in traffic flow. One of the representative CA model is Nagel-Schreckenberg (NS) model proposed in 1992 [19]. In NS model, cars move by four rules described as follows

R1 acceleration: $v_n^{t+1} \leftarrow \begin{cases} v_n^t + 1 & (v_n^t < v_{\mathrm{MAX}}) \\ v_n^t & \text{otherwise} \end{cases}$

R2 deceleration: $v_n^{t+1} \leftarrow \min\left(v_n^{t+1}, d_n^t\right)$

R3 random braking: $v_n^{t+1} \leftarrow \max\left(v_n^{t+1} - 1, 0\right)$ with probability p

R4 moving: $x_n^{t+1} \leftarrow x_n^t + v_n^{t+1}$,

where x_n^t and v_n^t are the location and velocity of the car n at time t respectively, and the car $n-1$ represents the car in front of the nth car. d_n^t is the gap between the car n and car $n-1$, that is $d_n^t = x_{n-1}^t - x_n^t - 1$. Because cars move no more than d_n^t in one time step, each of them is certified not to collide the car in front. In the rule R3, the randomization is introduced in order to cause the fluctuation of each car's velocity. NS model can reproduce both a free flow and a congestion flow.

Despite of the simplicity of NS model, it can be used to anticipate basic properties such as the occurrence of a jam in a location. Besides, CA model is easy to add the rules that cars obey on moving compared to fluid and car–following models. On the basis of the NS model, many CA model considering several effects on driving have been proposed and have been used for the investigation of the effect on the whole traffic flow [20–22].

Car following model

One of the familiar Car–following models proposed earlier is Gazis model [23] described as follows

$$\dot{v_i}\left(t+\tau\right) = a\left[v_{i-1}\left(t\right) - v_i\left(t\right)\right], \tag{1.1}$$

where $x_i\left(t\right)$ and $v_i\left(t\right)$ are the location and velocity of car i at time t respectively, and car $i-1$ represents the car in front of car i. Therefore each car determines its acceleration by the relative velocity to the car in front. Parameter a is defined as a sensitivity of a reaction of cars and is set to a positive value. It represents the strength of the influence by the changes of the relative velocity to the car's acceleration. τ is a drivers' reaction time. It is natural that it takes a certain period for human to recognize the change of relative velocity. In Eq. (1.1), if the relative velocity is positive i.e., $(v_i > v_{i+1})$, the right hand side of the equation becomes negative and the i th car decelerates. To the contrary, the car accelerates if the relative velocity is negative. These behavior is natural for the driving action. It should be noted that the term of reaction time makes the differential equation difficult to analyze the behavior of cars theoretically. In Ref. [23], the fundamental diagram was investigated with the model in the case where a is not only constant value but also depends on the relative distance $(x_i - x_{i+1})$.

As another familiar car–following model, Bando et, al. have proposed "*optimal velocity* (OV)" model [24]. In this model, a new function "*optimal velocity function*" is introduced to each car. Each car aims the velocity determined by the function. The equation is

described as follows

$$\dot{v_i}(t) = a\left[V(\Delta x) - v_i(t)\right], \tag{1.2}$$

where a is a sensitivity of the reaction of cars and V is the optimal velocity function. The function monotonously increases with the relative position to the preceding car Δx and it goes asymptotically to a maximal velocity as $\Delta x \to \infty$. The function is set to be considered for human's psychology of driving and the maximal velocity is considered for the restriction of the velocity caused by the performance of cars. Cars obeying this model keep a relative distance $\bar{\Delta x}$ and the velocity $\bar{v} = V\left(\bar{\Delta x}\right)$ in a uniform flow, which is the state where all cars move at the same velocity. In this model, the stability of a uniform flow against perturbations is analytically derived by the linear stability analysis. Figure 1.2 shows the stability and instability regions in a two-dimensional parameter diagram. The stability and instability regions is the region (i) and (ii), respectively. In the region (i), any perturbation decays and a uniform flow can be maintained. In the region (ii), on the other hand, some perturbations grow and eventually the uniform flow is collapsed. In this case, there coexist two clusters of cars, that of cars moving at a high velocity and others moving at a low velocity. The boundary line between (i) and (ii) is described as the equation

$$a = 2V'\left(\bar{\Delta x}\right), \tag{1.3}$$

where $V'\left(\bar{\Delta x}\right)$ is the value of V differentiated with Δx and substituted $\bar{\Delta x}$ into. If $a > 2V'\left(\bar{\Delta x}\right)$, the uniform flow is stable against any perturbation.

Other than there car–following models, one of model often used in a control engineering is Helly model [25]. The model is described as follows

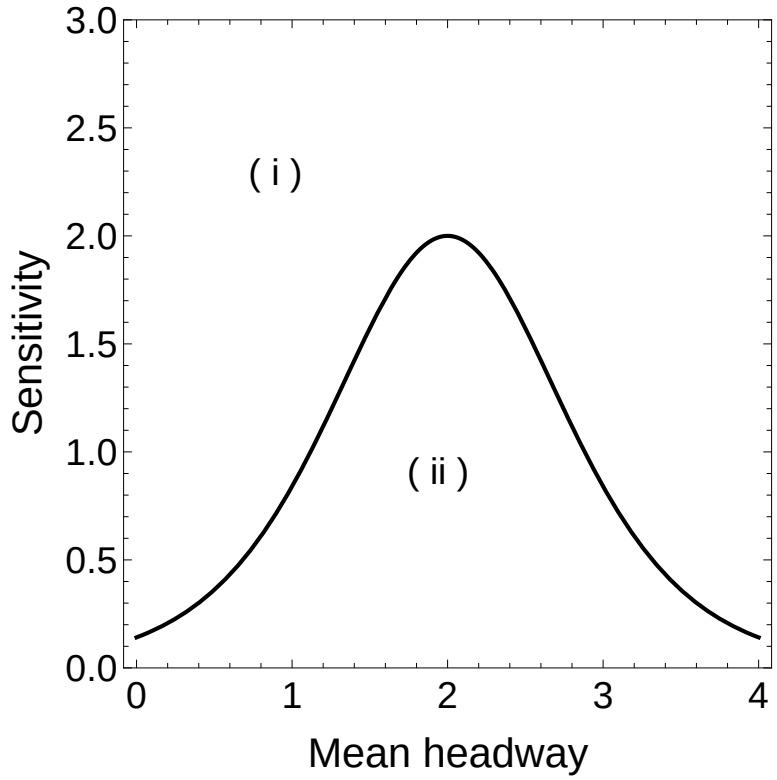

Fig. 1.2. The linear stability condition of OV model. We use $\tanh(\Delta x - 2) + \tanh 2$ as the equation of $V(\Delta x)$, which is identical with Eq. (24) in Ref. [24]

$$\dot{v}_i(t+\tau) = k_1\left[x_{i-1}(t) - x_i(t) - D_i(t)\right] + k_2\left[v_{i-1}(t) - v_i(t)\right] \tag{1.4}$$

$$+k_3 B_{i-1} + k_4 B_{i-2}, \tag{1.5}$$

$$D_i(t) = \alpha + \beta v_i(t) + \gamma \dot{v}_i(t), \tag{1.6}$$

$$B_{n-1} = \begin{cases} 0 & \text{if car } i-1 \text{ is not braking} \\ 1 & \text{if car } i-1 \text{ is braking,} \end{cases} \tag{1.7}$$

$$B_{n-2} = \begin{cases} 0 & \text{if car } i-2 \text{ is not braking} \\ 1 & \text{if car } i-2 \text{ is braking,} \end{cases} \tag{1.8}$$

where $x_i(t)$ and $v_i(t)$ are the location and velocity of car i at time t respectively, and car $i-1$ represents the car in front of car i. Each car determines the value of acceleration in response to the relative position and velocity of the car in front. k_1 and k_2 are the sensitivities toward the relative distance and velocity, respectively. D_i is car i's desired gap and depends on v_i and $\dot{v}_i$. The parameter α in D_i is the desired gap in a halting

state. It should be noted that each car's desired gap includes the length of the car. k_3 and k_4 are the coefficients of the brake factors of car $i-1$ and car $i-2$, respectively. Due to the factors, the behavior of each car is affected by brake lamps of the preceding cars. In a uniform flow, each car keeps a common velocity $v(t) = \bar{v}$ and a common gap $D_i = \alpha + \beta\bar{v}$.

Here, we explain the stability of the uniform flow composed of cars obeying the Helly model [Eq. (1.5)] with omitting the time delay τ, the brake factors and the term of $\dot{v}_i$ in D_i for simplicity. We describe the simplified Helly model as follows

$$\dot{v_i}(t) = k_1 \left[x_{i-1}(t) - x_i(t) - D_i(t)\right] + k_2 \left[v_{i-1}(t) - v_i(t)\right], \tag{1.9}$$

$$D_i(t) = d + T_{\mathrm{des}} v_i(t), \tag{1.10}$$

where in D_i is the desired gap in a halting state (corresponds to α in [Eq. (1.5)]) and T_{des} corresponds to the target inter-vehicular time. A target inter-vehicular time of a car is defined as a period from when the preceding car's tail passes a certain position to when the car's head passes the position. Each car's desired gap is the function of v_i and can be written in the notation, $D_i = D(v_i) = d + T_{\mathrm{des}} v_i$. In the simplified Helly model, the stability of the uniform flow can be derived analytically with the string stability. The string stability is defined to a column of cars composing of a flow (Note that it is defined even if the flow is not a uniform flow.) and judged whether a fluctuation of the tail car of the column is smaller than that of the head car of the column. If the fluctuation of the tail car is equal to or smaller than that of the head car, the column shrinks the perturbation caused by the head car and translates the shrunken perturbation to the tail car. In this case, the column is defined to satisfy the string stability condition. On the other hand, if the fluctuation of the tail car is larger than that of the head car, the column amplifies the perturbation caused by the head car and translates the amplified perturbation to the tail car. In this case, the column does not to satisfy the string stability condition. In a uniform flow with a common velocity $\bar{v}$ and a common gap $D(\bar{v})$ obeying the Helly model expressed in Eqs. (1.9) and (1.10), the string stability condition is known [26], which is described by the following inequality

$$T_{\mathrm{des}} \geq \frac{-k_2 + \sqrt{{k_2}^2 + 2k_1}}{k_1}. \tag{1.11}$$

The calculation process of the stability condition in the Helly model is explained in detail

in Appendix A.1.

1.2.2 Studies for solving traffic jam

Strategies for traffic jam are categorized into macroscopic approaches and microscopic approaches. The macroscopic strategies, as mentioned in the section 1.1, aim to avoid the excessive density by restricting the inflow of cars. These strategies have been proposed in the field of traffic engineering and operated such as ramp metering [27, 28], variable speed limits (VSL) [29–31] and congestion pricing [32–34]. Ramp metering is operated in an intersection or a ramp in highway. VSL restricts the maximal velocity on highway dynamically depending on the scale of the congestion. Congestion pricing forces drivers to pay an extra tall to pass a certain highway in a certain period such as rash hour. On the other hand, in the the strategies based on microscopic car behaviors, a jam is prevented from growing by introducing car's which satisfy the stability condition mentioned in the section 1.2.1. These strategies have been studied in the field of physics, separately from that of traffic engineering. One effective development in this microscopic scope is the adaptive cruise control (ACC) [35], an on-board system that controls time-headways and velocities with a headway sensor, enabling the car to adopt car-following behaviors more accurately than is possible by human driving. The efficiency of ACC in preventing traffic jams has been reported through several numerical simulations [36–38] and experiments with real cars [39–41]. Although ACC as a microscopic strategy for solving traffic jam has a high potential to ease traffic jams, ACC is yet to gain widespread use; among standard-size cars manufactured in 2010 for use in Japan, only 2.8% $(122,750/4,377,953)$ were equipped with ACC (ACC in full range speed) [42]. This penetration rate is much smaller than the penetration rates succeeding in suppressing traffic jams predicted by numerical simulations: 20 % [36, 37] and 25 % [38].

The problem comes from the dynamical driving in ACC. The car equipped ACC has a characteristic of pursuing dynamically the preceding car all the time. Due to the characteristic, for a single car, the behavior does not affect greatly the whole traffic flow. Therefore, the whole traffic flow is possibly changed greatly by the behavior of a few cars tuning dynamic ON and OFF.

As this strategy based on the driving tuning dynamic ON and OFF, Beaty discussed how a traffic jam changes if a car does not pursue the preceding car but takes a large headway before encountering the traffic jam in advance [43]. If the car has a quite larger

headway than its desired headway, even if the preceding car is involved a jam, the car can keep a constant speed with consuming the large headway. While keeping a large headway, the car's behavior is not influenced by the jam. According to Beaty, if a car catches up with the preceding car in the right timing, its followers can avoid braking, i.e., the jam is removed. The advantage of Beaty's method is that a jam is removed by a single car. However, Beaty's driving method lacks theoretical supports; for instance, the appropriate headway distance required for removing jam is not derived. Recently, a theoretical framework based on a simple model has been developed which demonstrates the ability of a single car to remove a jam [44]. The method in the theory is called "*jam-absorption driving*", and in this paper, we abbreviate the jam-absorption driving to "JAD". The name of jam-absorption is derived from the behavior of a single car which is not influenced a jam entirely and passes through as if no jam occurs from the beginning. Cars that perform JAD ("*absorbing cars*") undertake a chain of two actions, "*slow-in*" and "*fast-out*". Slow-in allows the car to circumvent a jam, and remove it by decelerating and enlarging its own headway in advance. Fast-out is performed after slow-in, and involves following the car in front with sufficient acceleration to prevent time delay. Consecutive applications of the two actions are expected to prevent the following cars from falling into the so-called "*memory effect*", the prolonged net time-gaps after staying in a jam [45, 46]. On the other hand, JAD itself causes perturbations such as compression and expansion waves due to its irregular motion (See Fig 2.1 in chapter 2). The theory predicts the condition under which a jam can be removed without forming the so-called "secondary jam." Under this condition, the compression and expansion waves caused by the absorbing car intercept and cancel out. The explicit form of this meeting point in a time-space diagram can be derived from the theory, and the trajectory of this point can be altered by changing the slow-in timings.

1.3 Purpose of the study

We only know about the new theory JAD the theoretical analysis using a simple model and we need to discuss the effect of JAD on the traffic jam from several aspects such as numerical simulations and experiments. In this study, we investigate and report the effect of JAD in numerical simulations and an experiment. We introduce a car-following model which does not considered in the previous study of JAD and classify the condition of the behavior of the absorbing car to remove a jam and avoid a secondary jam with the

simulations. Furthermore, we experimentally demonstrates JAD with human driving cars to confirm that JAD does not worsen the traffic flow. Then, to observe the effect of JAD in real driving situations,

1.4 Composition of this paper

This paper is composed as follows. We have already explained the mechanism of the traffic jam and models to reveal the mechanism briefly and have introduced the previous studies for solving traffic jam as the introduction in chapter 1. Then, we explain the description of the strategy proposed in Ref. [44] in chapter 2. In chapter 3, we conduct the numerical simulations of JAD and describe the result. Section 4 is the results of our experiment. In the end, we conclude the findings in chapter 2, 3 and 4 and discuss potential future works in section 5.

Chapter 2

Theory of JAD

2.1 Strategy of JAD

JAD is performed in a situation where a jam occurs in the downstream direction of the absorbing car and is propagating toward the car as shown in Fig. 2.1. In this situation, a jam occurs and develops by catching cars. The caught cars stop in order of the column. The action of JAD is mentioned as follows. As the first step of JAD, the absorbing car decelerates and keeps its velocity in advance before the jam reaches it (slow–in). By slow–in, the absorbing car enlarges its inter-vehicular distance. When the preceding car of the absorbing car is involved in the jam and stops, because the absorbing car maintains a large gap, it is not involved in the jam but does keep its velocity. Then, as the second step of JAD, when the preceding car comes out of the jam and changes its velocity at a high speed, the absorbing car changes its velocity at the high speed (fast–out). Due to these actions of JAD, the absorbing car is not forced to stop by the jam and can intercept the propagation of the jam.

In this situation, the cars behind the absorbing car are affected by the behavior of JAD. Due to their behaviors affected by JAD, the compression wave and expression wave occur and propagate to them. In the study of Ref. [44], secondary jams do not occur if the two waves intersect. JAD has the strategy aiming at the intersection of the two waves.

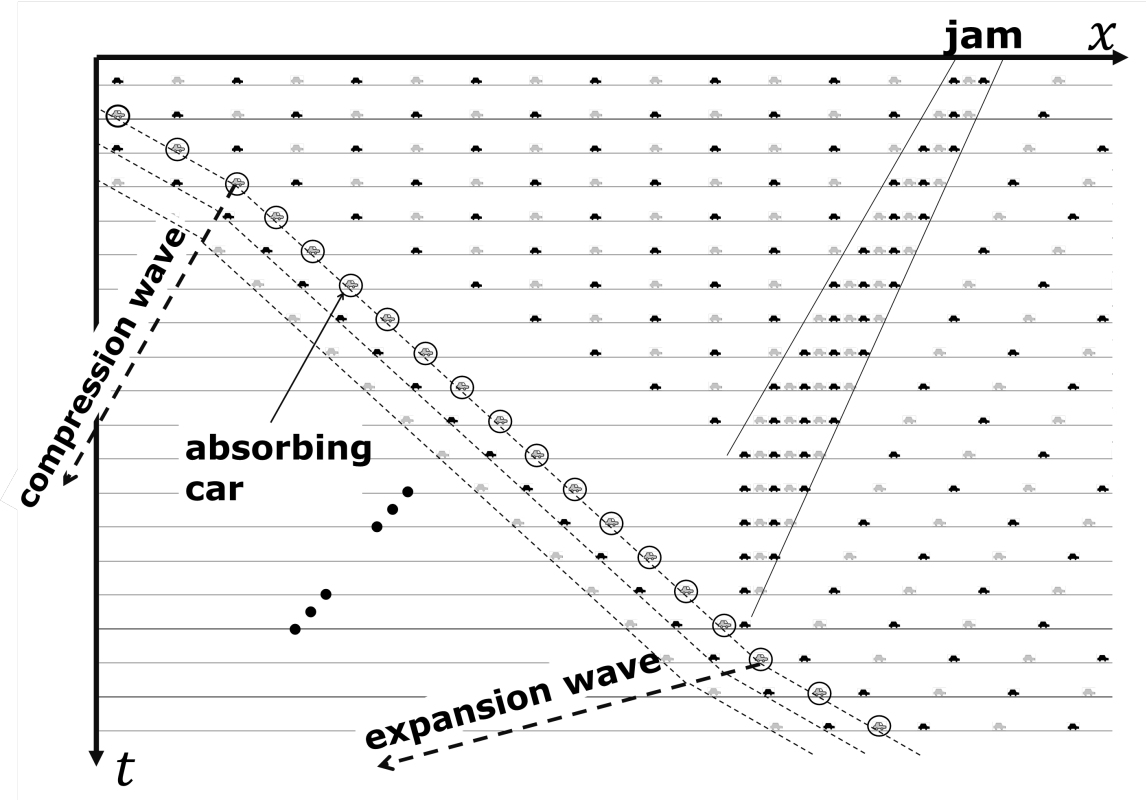

Fig. 2.1. Schematic view of the slow-in and fast-out performed by the absorbing car. The horizontal and vertical axes correspond to the position and the time, respectively. The circled icons represent the absorbing car. The cars behind the absorbing car follow it. The compression and expansion waves occur due to the slow-in and fast-out, respectively.

2.2 Model for traffic flow

We describe the simple microscopic car behavior model used in the jam–absorption theory in Ref. [44]. In the model, each car's velocity depends on the gap to the car in front. The velocity v is determined according to the following equation

$$v = \begin{cases} \left(\dfrac{h-d}{l-d}\right)^m v_{\mathrm{MAX}} & d \le h \le l, \\ v_{\mathrm{MAX}} & h \ge l, \end{cases} \tag{2.1}$$

where h is the gap of each car to the car in front, and d is the sum of the gap and the length of the car in the halting state. v_{MAX} is the maximal velocity of cars and l is the minimal gap which cars can maintain at the velocity v_{MAX}. When a car's gap is smaller than l, the velocity of the car changes into a smaller value than v_{MAX} by obeying Eq. (2.1). Here, m is

the parameter which controls the degree of the velocity variation. It should be noted that each car does not consider the acceleration and changes its velocity immediately. With Eq. (2.1), the relationship between the traffic density and flux composed of by massive cars can be calculated. The fundamental diagram of the traffic flow can be drawn in Fig. 2.2. The free flow and congestion flow can be expressed. In both cases of the parameter $m > 1$ and $m < 1$, the curves corresponding to the congestion flow are convex ones. In the scenario mentioned as follows, the scale of a jam growth does not depend on the value of m. Therefore, in this paper, we discusses the effect of JAD on the traffic jam in the case of $m = 1$ for simplicity.

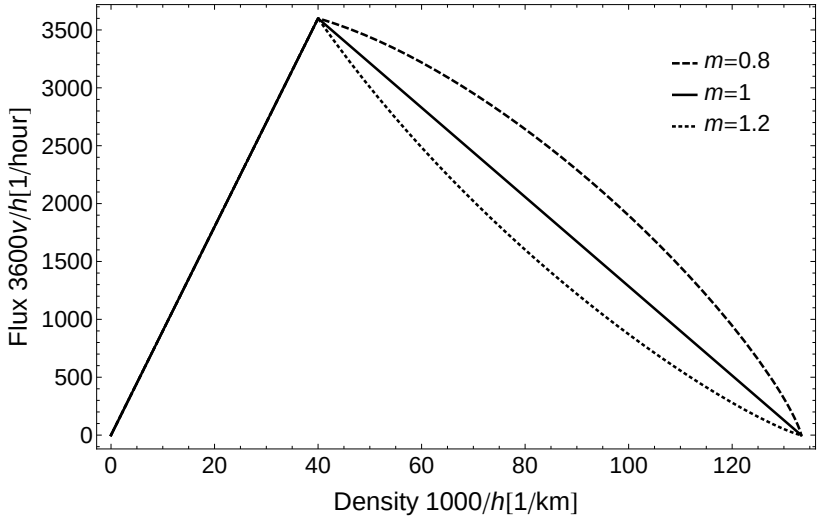

Fig. 2.2. Fundamental diagram calculated with the relationship between the velocity v and the gap of cars h described by the Eq. 2.1. The density and the flow are described as $\frac{1000}{h}$ [1/km] and $\frac{3600v}{h}$ [1/hour], respectively. The gap h is changed from $d = 7.5$ [m] to a sufficiently large value such as 10000 [m]. In the diagram, l and v_{MAX} are set to 25 [m] and 25 [m/s], respectively. If $h > l$, the lines in all cases of $m = 0.8$, $m = 1.0$, $m = 1.2$ overlap each other. On the other hand, if $d < h < l$, the lines in the cases of $m = 0.8$ and $m = 1.2$ are bended. In all cases, the flows at the point of $h = d$ are the same each other.

Here, we explain a scenario where a jam develops and propagates to the upstream direction by using the simple car following model (Fig. 2.3). The scenario is described as follows: All cars keep the velocity with v_{MAX} and the gap with h_1 ($h_1 > l$). At a time, a car located in the downstream direction (called car 1) stops for a period T and then changes the velocity into v_{MAX}. Car 1's action causes a perturbation and it propagates to the following cars. Each of the following cars keeps v_{MAX} until its gap becomes d, and then it changes its velocity into 0 and have the gap d. After a halting state, the car changes its velocity into v_{MAX} when the gap of the car is enlarged to h_2 ($> h_1$). The

enlargement of the gap is caused by the memory effect.

We analytically investigate the characteristics of the compression and expansion waves due to the perturbation caused by the car 1. The two waves can be obtained as lines by connecting the collective points on which each car's trajectory are bended in the time–space diagram. It should be noted that both the two waves do not have their width in the simple model. The propagation speeds of the compression and expression waves are defined as the parameter v_S and v_R, respectively. They can be calculated as the gradients of the lines as follows

$$v_S = \frac{0 - v_{\mathrm{MAX}}/h_1}{1/d - 1/h_1} = -\frac{dv_{\mathrm{MAX}}}{h_1 - d}, \tag{2.2}$$

$$v_R = \frac{0 - v_{\mathrm{MAX}}/h_2}{1/d - 1/h_2} = -\frac{dv_{\mathrm{MAX}}}{h_2 - d}. \tag{2.3}$$

From Eqs. (2.2) and (2.3), if $h_1 < h_2$, $v_S < v_R$ is satisfied thus the jam grows. With using the equation $v_S(t_A - t_G + T) = v_R(t_B - t_G) = -(N_1 - 1)d$, we can calculate the position x_A and the time t_A at which a car located in $N_1 - 1$ th behind the car 1 (car N_1) is involved in the jam as follows

$$x_A - x_G = -(N_1 - 1)d, \tag{2.4}$$

$$t_A - t_G = -T - \frac{(N_1 - 1)d}{v_S} = -T + \frac{(N_1 - 1)(h_1 - d)}{v_{\mathrm{MAX}}}, \tag{2.5}$$

$$\tag{2.6}$$

where x_G and t_G are the position and time at the point G in the Fig. 2.3, which represents the states in which the car 1 changes the velocity into 0 and halts. As well as x_A and t_A, x_B and t_B at which car N_1 comes out of the jam can be calculated as

$$x_B - x_G = -(N_1 - 1)d, \tag{2.7}$$

$$t_B - t_G = -\frac{(N_1 - 1)d}{v_R} = \frac{(N_1 - 1)(h_2 - d)}{v_{\mathrm{MAX}}}. \tag{2.8}$$

Therefore, the period for which the car N_1 is involved in the jam is calculated as

$$t_B - t_A = T + \frac{N_1 - 1}{v_{\mathrm{MAX}}}(h_2 - h_1). \tag{2.9}$$

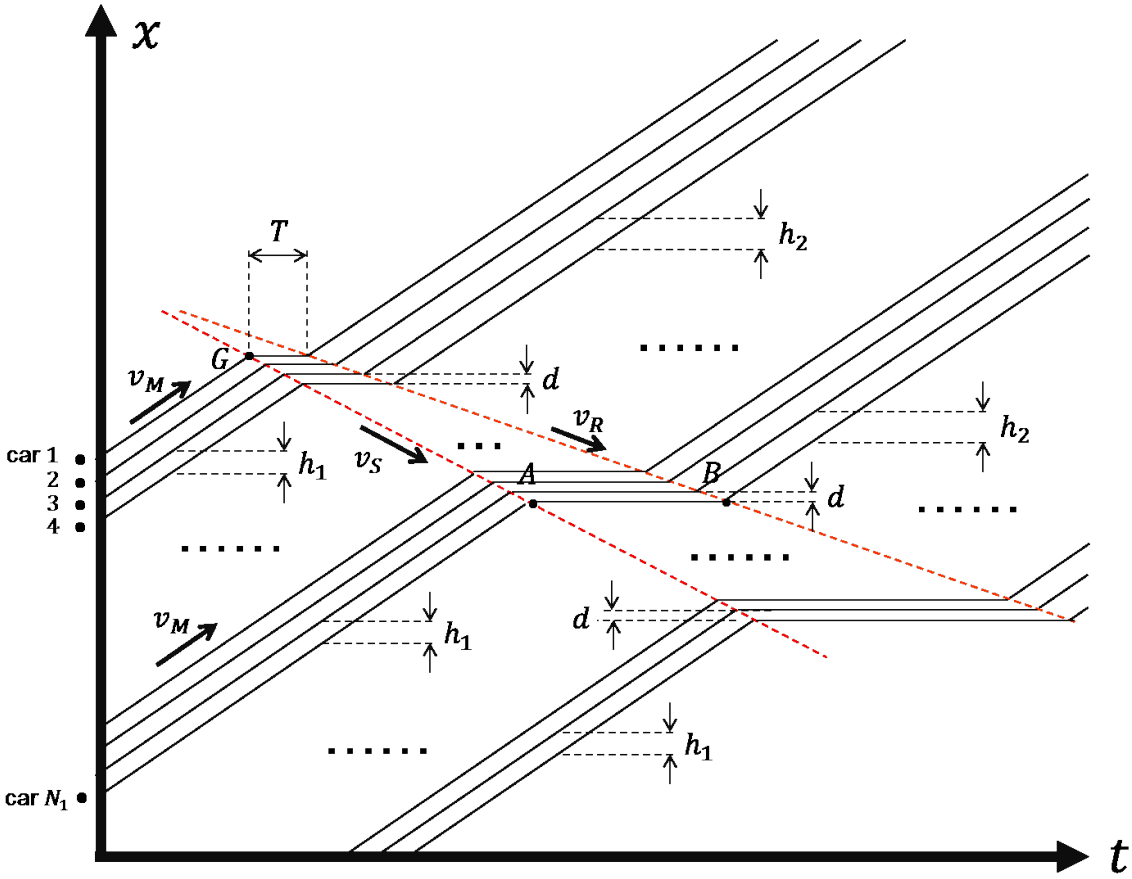

Fig. 2.3. Time–space diagram of a traffic flow reproduced by a simple car behavior model in Ref. [44]. The horizontal and vertical axes correspond to the time and the position, respectively. Each line represents the trajectory of a car and its gradient at a time corresponds to the velocity at the time. The horizontal line of each trajectory represents the halting state of the car.

2.3 Theoretical analysis

Here, we analytically investigate the influence of JAD on the jam in the simple car behavior model with JAD. To discuss it, we introduce a scenario described as follows. The initial state and the action of car 1 is the same as those in the scenario without JAD. We assign car $N_1 + 1$ to the absorbing car. The behavior performed by the absorbing car is drawn in Fig. 2.4. As the first step of JAD, the absorbing car performs slow–in and changes its velocity into v_a ($< v_{\mathrm{MAX}}$) when it passes a point C in the diagram. It aims to pass the point D in the diagram, which is the point of the states where the absorbing car's gap is d when the car N_1 comes out of the jam. As the second step of JAD, the absorbing car performs fast–out (changes its velocity into v_{MAX}) when it passes the point E in the diagram, which is the point of the states where the absorbing car keeps the velocity v_a and its gap is l. We denote the period for which the absorbing car performs slow–in from the point C to the point E as T_a. In this situation, T_a and v_a have an relationship described as the following equation

$$T_a = \frac{Tv_{\mathrm{MAX}} + (N_1 - 1)(h_2 - h_1) - (h_1 - l)}{v_{\mathrm{MAX}} - v_a}. \tag{2.10}$$

x_C, t_C, x_E and t_E are described with v_a as follows

$$t_C - t_G = \frac{1}{v_{\mathrm{MAX}} - v_a}\left(-Tv_{\mathrm{MAX}} + (N_1 - 1)(h_1 - d) + h_1 - \frac{v_a}{v_{\mathrm{MAX}}}(N_1 - 1)(h_2 - d) - d\right), \tag{2.11}$$

$$t_E - t_G = \frac{(N_1 - 1)(h_2 - d)}{v_{\mathrm{MAX}}} + \frac{l - d}{v_{\mathrm{MAX}} - v_a}, \tag{2.12}$$

$$x_C - x_G = -(N_1 - 1)d - h_1 - \frac{v_{\mathrm{MAX}}}{v_{\mathrm{MAX}} - v_a}\left(\frac{v_a}{v_{\mathrm{MAX}}}(N_1 - 1)(h_2 - h_1) + v_aT - h_1 + d\right), \tag{2.13}$$

$$x_E - x_G = -(N_1 - 1)d - \frac{v_{\mathrm{MAX}}d - v_al}{v_{\mathrm{MAX}} - v_a}. \tag{2.14}$$

The following cars of the absorbing car also change the velocities into v_a affected by slow–in. The timing of changing into v_a is that when each car's gap is h_3, which is obtained

by substituting v_a into Eq. (2.1) as follows

$$h_3 = d + \frac{v_a}{v_{\mathrm{MAX}}} (l - d) . \tag{2.15}$$

Then each car changes the velocity into v_{MAX} when its gap is l. Note that the memory-effect does not occur to the cars in this situation because they are not involved in a jam. As well as the perturbations caused by the car 1, JAD also causes the compression and expression wave. The velocity of the compression wave v_b and the expression wave v_c are calculated as the following equation

$$v_b = \frac{v_a/h_a - v_{\mathrm{MAX}}/h_1}{1/h_a - 1/h_1} = \frac{v_a h_1 - v_{\mathrm{MAX}} h_a}{h_1 - h_a} \tag{2.16}$$

and

$$v_c = \frac{v_a/h_a - v_{\mathrm{MAX}}/l}{1/h_a - 1/l} = \frac{v_a l - v_{\mathrm{MAX}} h_a}{l - h_a}, \tag{2.17}$$

respectively. If $v_b > v_c$, the two waves intersect in a certain position in the upstream direction from the position of the absorbing car. We define the point in time–space diagram where the two waves intersect as F, and denote the certain position and the certain time as x_F and t_F, respectively. We also define the car which moves just behind the position x_F at t_F as car N_2. In this case, car N_2's gap is always above h_3 even if it keeps the velocity v_{MAX}. Thus, car N_2 and the following cars can keep the velocity v_{MAX} and the two waves disappear, i.e., the jam which develops and propagates to the absorbing car is absorbed by its following cars and finally disappears. By using the inequality $v_b > v_c$ with substituting Eq. (2.16) into v_b and Eq. (2.17) into v_c, we can obtain the condition of jam absorption described as

$$h_1 > l \tag{2.18}$$

Here, we assume the inequality (2.18). With the assumption, we calculate the point F and the number of cars which is required to absorb the jam. The position x_F and the

time t_F are calculated as

$$t_F - t_G = \frac{v_a}{(v_{\mathrm{MAX}} - v_a)\, v_{\mathrm{MAX}}} (l - d) + \frac{1}{(h_1 - l)\, v_{\mathrm{MAX}}} \left(T v_{\mathrm{MAX}} (l - d) + (N_1 - 1)(h_1 - d)(h_2 - l)\right), \tag{2.19}$$

$$x_F - x_G = -\frac{d}{h_1 - l} \left(T v_{\mathrm{MAX}} + (N_1 - 1)(h_2 - h_1)\right) + \frac{v_a}{v_{\mathrm{MAX}} - v_a} (l - d) - (N_1 - 1)\, d. \tag{2.20}$$

We can obtain a relationship between t_F and x_F by uniting Eq. (2.19) and Eq. (2.20), and deleting $\frac{v_a}{v_{\mathrm{MAX}} - v_a}$ from them as follows

$$x_F - x_G = (t_F - t_G)\, v_{\mathrm{MAX}} - \frac{1}{h_1 - l} \left(T v_{\mathrm{MAX}} l + (N_1 - 1)(h_2 - l)\, h_1\right). \tag{2.21}$$

In the time–space diagram, the line obtained from Eq. (2.21) has gradient v_{MAX} (Fig. 2.5). Thus the line is depicted in parallel with the trajectories of the car N_2 and is located between the trajectories of the car $N_2 - 1$ and car N_2. Therefore, the number N_2 does not depend on v_a.

Suppose N_2 is a sufficiently large value, $x_G - x_F \mid_{t_F = 0}$ approximately equals to the relative position of the car N_2 at time 0 to x_G. The relative position is calculated as the sum of the gaps from car 1 to car N_2. Thus the relationship is derived as follows

$$x_G - x_F \mid_{t_F = 0} \approx (N_2 - 1)\, h_1. \tag{2.22}$$

N_2 can be calculated from Eq. (2.21) and Eq. (2.22) as follows

$$N_2 \approx \frac{1}{h_1 - l} \left(\frac{l}{h_1} T v_{\mathrm{MAX}} + (N_1 - 1)(h_2 - l)\right) \tag{2.23}$$

Suppose that both N_1 and N_2 are sufficiently large, the number of cars which is required to absorb the jam $N_2 - N_1$ is in proportion to N_1 and the proportion $\frac{N_1 - N_2}{N_1}$ is

$$\frac{h_2 - l}{h_1 - l} - 1 = \frac{h_2 - h_1}{h_1 - l}. \tag{2.24}$$

Moreover, both t_F and x_F can be regarded as linear functions of $\frac{v_a}{v_{\mathrm{MAX}} - v_a}$. Because $\frac{v_a}{v_{\mathrm{MAX}} - v_a}$ monotonously increases with v_a, the point F moves to the right direction in the time-space diagram as shown in Fig. 2.5 as v_a increases. In the case of $v_a = 0$, t_F and x_F

are described as

$$t_F \mid_{v_a=0} - t_G = \frac{1}{(h_1 - l)\, v_{\mathrm{MAX}}} \left(T v_{\mathrm{MAX}} (l - d) + (N_1 - 1)(h_1 - d)(h_2 - l) \right), \tag{2.25}$$

$$x_F \mid_{v_a=0} - x_G = -\frac{d}{h_1 - l} \left(T v_{\mathrm{MAX}} + (N_1 - 1)(h_2 - h_1) \right) - (N_1 - 1)\, d. \tag{2.26}$$

In the case of $v_a \to v_{\mathrm{MAX}}$, both t_F and x_F go to infinity. Note that in the case of $v_a = 0$, although the memory effect must occur to the cars from the car $N_1 + 1$ to the car N_2, the point F in this case represents the case without the effect.

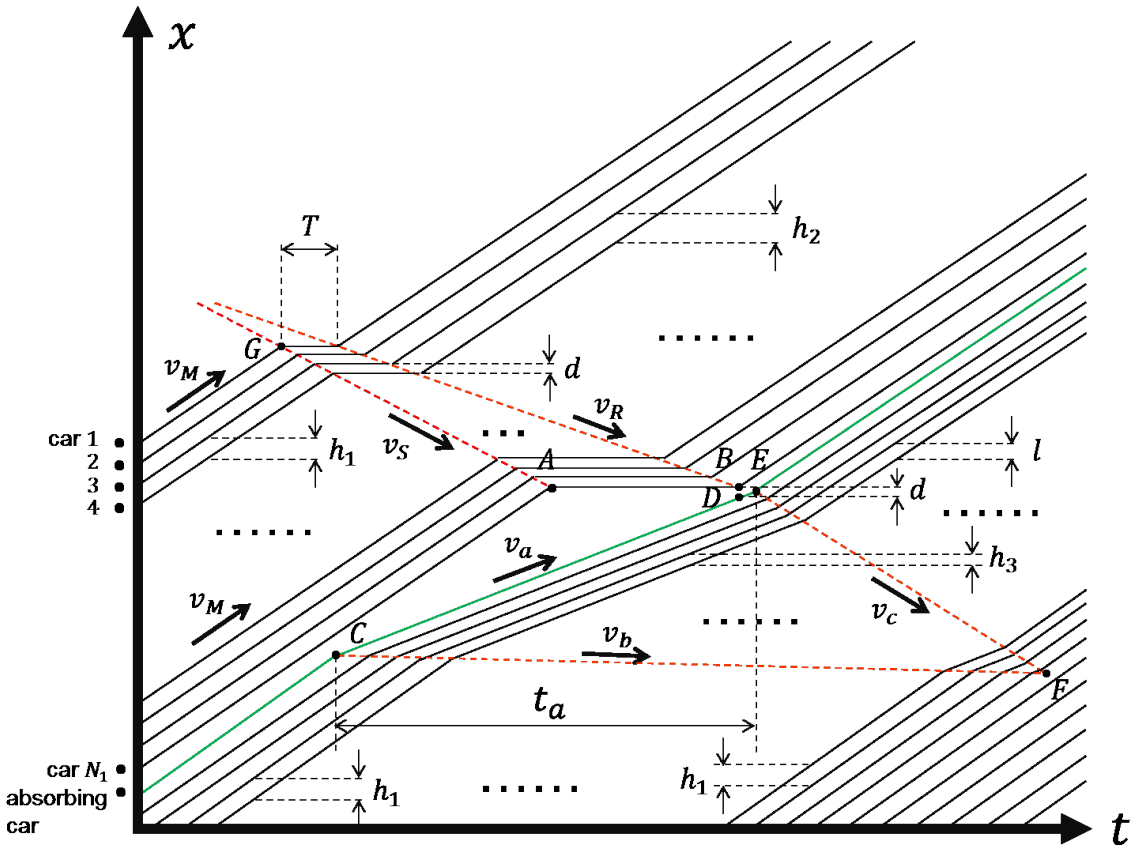

Fig. 2.4. Time–space diagram representing a situation where the absorbing car performs JAD to remove a jam propagating from the downstream direction. Each line is the trajectory of a car. The green one is that of the absorbing car. The absorbing car starts slow–in at the point C. It aims at the point D and then ends slow–in and starts fast–out immediately after passing the point E. The compression and expansion waves caused by JAD are drawn by the line segment CF and EF, respectively. The velocities of the compression and expansion waves are denoted by v_b and v_c, respectively. Because of JAD, the memory effect does not occur to the following car of the absorbing car and v_c becomes smaller due to the absence of the effect. In this situation, $v_b > v_c$ is satisfied and the two waves intersect and finally disappear.

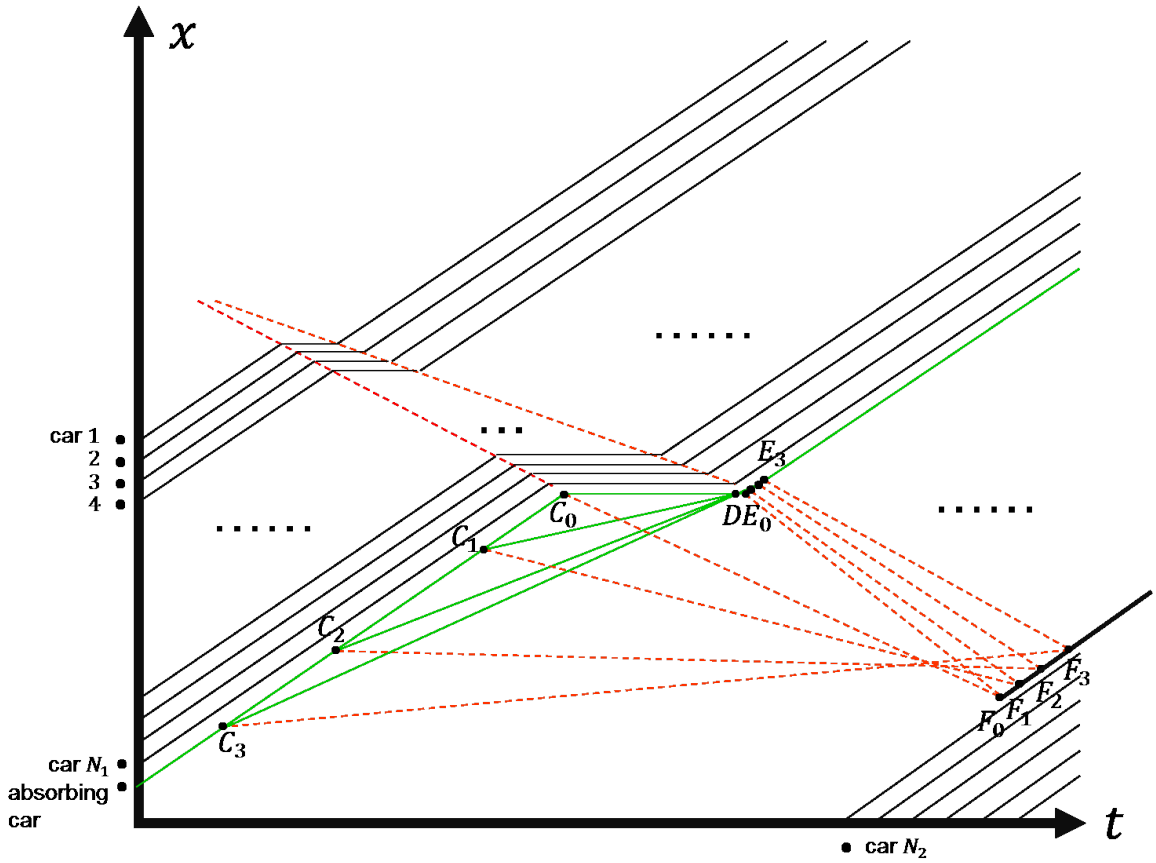

Fig. 2.5. JAD with various v_a in the kinematic–like model. As examples of patterns of JAD with various v_a, we draw four patterns of JAD with changing v_a. In each pattern of JAD, the absorbing car starts slow–in at the point C_i and aims at the point D, then ends slow–in and starts fast–out after passing the point E_i, where i has the value of 0, 1, 2 and 3. Here, v_a is equal to 0 in the case of $i = 0$ and it becomes larger as i increases. Each line segments C_iF_i and E_iF_i represent each compression and expansion waves,respectively. F_i is the vanishing point of the two waves in each pattern of JAD. The bold half line which starts from F_0 corresponds to the trajectory of F with changing v_a from 0 to v_{MAX}.

2.4 Conclusion

The jam–absorption theory in Ref. [44] aims at the construction of theoretical framework in order to bring a simple comprehension to the effect of JAD on a traffic jam. The theory expresses a traffic flow composed of massive cars with a simple microscopic car behavior model and formalizes the behavior of JAD in the situation where a jam occurs and propagates to the upstream direction. In that study, the behaviors of the compression and expansion waves caused by JAD were analytically investigated. In this paper, we introduce the results of the analysis of the behaviors in that study with the parameter m restricted to 1. One important findings from the results is that the condition of the disappearance of jam is $h_1 > l$. This condition means JAD succeeds if it is performed in advance when the traffic density is smaller than the critical density. The other important one is that the number of cars which is required to absorb the jam $N_2 - N_1$ does not depend on the velocity v_a. The study in Ref. [44] does not investigate the behavior of the two waves only for $m = 1$ but also for $m < 1$ and $m > 1$. In these cases, the study confirms the same condition of the disappearance of jam with the case of $m = 1$ and the independence of $N_2 - N_1$ on v_a as wall as the case of $m = 1$. These results bring a simple comprehension of the influence of JAD on the traffic flow. Thus the study concludes that the theoretical framework is accomplished to be constructed.

It is a new idea that a car removes a jam by avoiding the occurrence of the memory effect. However, this theory uses a very simple car behavior model so that it is unclear JAD method is available to remove the jam in real highway traffic. Therefore, as the next step, it needs to study the effect of the JAD method on a traffic flow with numerical simulations by using a more realistic car behavior model in anticipation of application.

Chapter 3

Numerical simulation of JAD

3.1 Introduction

JAD is composed of two actions: "*slow-in*" and "*fast-out*," as shown in Fig. 2.1 in Chap. 2. Slow-in consists of keeping a large headway to avoid being involved in a traffic jam. The traffic jam is removed because of this large headway. Fast-out is performed after slow-in and consists of following the car in front, which has exited from the traffic jam, with a short headway. The theory considers the so-called "*memory effect*" (or "*frustration effect*") [45, 46], which is the enlargement of the net time gap after being involved in a traffic jam and which causes the growth of traffic jams. Cars following the absorbing car avoid being involved in a traffic jam by JAD. Therefore, the memory effect is not expected to occur for these cars. Thus, JAD prevents the aggravation of the car-following behavior of the following cars. However, because of its irregular motion, JAD itself causes perturbations such as compression and expansion waves (Fig. 2.1). In the framework of this theory [44], the compression and expansion waves should collide with each other and disappear to avoid the so-called "*secondary traffic jams.*" The theory indicates that a headway threshold exists that prevents secondary traffic jams.

The theory [44] does not consider some points. The first is that it does not consider the accelerations of cars. The second is the lack of the stability of traffic flow, which determines whether secondary jams occur. The stability of traffic flow is closely related to the magnitude of perturbations. Below the critical density, there is a density region in which a perturbation grows if its amplitude exceeds the critical amplitude observed in macroscopic [14, 16], microscopic car-following [47] and cellular automaton [48] traffic models. In addition, Bando et al. concluded from a microscopic car-following traffic model that density ranges exist where homogeneous flow and congested flow coexist [24]. Moreover,

Helbing and Moussaid analytically calculated the critical amplitudes of perturbations in a microscopic car-following traffic model [49]. Based on these studies, we do not expect secondary jams to occur if the perturbations caused by the absorbing car are sufficiently small. According to these previous studies, we anticipate that in traffic flow composed of cars obeying a car-following model and maintaining extra-large gaps instead of minimal headway, traffic-flow stability depends on the magnitude of perturbations.

In this paper, we construct a framework of JAD that takes into account accelerations of cars and stability of traffic flow by introduction of car-following behaviors. First, we use a microscopic car-following model to numerically verify how the stability of traffic flow depends on the magnitude of perturbations. Next, we verify that a parameter region exists where the absorbing car avoids a traffic jam and prevents the growth of secondary jams. We also show that the validity of JAD is not influenced by the choice of a acceleration parameter value and a car-following model.

3.2 Model

Among the numerous car-following models proposed in the last several decades [4, 5, 9–11], simple classical models are sufficient for confirming that the stability of traffic flow depends on the magnitude of the perturbations. For a simple model, we use the Helly model [25], which is described by a set of linear differential equations

$$\dot{v_i}(t) = k_1 \left[x_{i-1}(t) - x_i(t) - D_i(t)\right] + k_2 \left[v_{i-1}(t) - v_i(t)\right], \tag{3.1}$$

$$D_i(t) = d + T_{\mathrm{des}} v_i(t), \tag{3.2}$$

where $x_i(t)$ and $v_i(t)$ are the location and velocity of the car i at time t, and the car $i-1$ represents the car in front of car i. Each car determines its own acceleration in response to the relative position and velocity of the car in front. The quantities k_1 and k_2 are the sensitivities to relative distance and velocity, respectively. $D_i(t)$ is the desired gap for car i and d is the desired gap when the car is stopped. T_{des} is the target intervehicular time. The target intervehicular time of a car is defined as the time period between when the preceding car's tail passes a certain position to when the car's head passes the same position. Note that, for simplicity, we ignore time delay, brake factors, and the term of $\dot{v}_i$ in D_i that were defined in the original Helly model [25]. Each car's desired gap is the function of v_i and can be written as $D_i = D(v_i) = d + T_{\mathrm{des}} v_i$. In the Helly model, uniform

flow can be attained, in which each car keeps a common velocity $v(t) = \bar{v}$ and a common gap $D(\bar{v}) = d + T_{\mathrm{des}}\bar{v}$.

However, the Helly model has unrealistic behavior. If a car gap is infinitely long, it continues to accelerate and its velocity reaches infinity. To avoid such behavior, we limit each car's velocity to the range $0 \leq v(t) \leq v_{\mathrm{MAX}}$, where v_{MAX} is the maximum velocity.

The Helly model is good for analyzing the stability of uniform flow by "*string stability*" [26]. In a flow composed of a column of cars, a perturbation, such as the leading car braking, propagates toward the following cars. Depending on the situation, a chain of responses of the following cars may grow to produce a traffic jam. If the braking of each car is less than or equal to the braking of the car in front, the perturbation is not amplified as it propagates toward the following cars. In this case, the flow satisfies the string-stability condition. However, if the braking of each car is greater than the braking of the car in front, the perturbation grows. In this case, the flow does not satisfy the string-stability condition.

In uniform flow obeying the Helly model [Eqs. (3.1) and (3.2)] and with a common velocity $\bar{v}$ and a common gap $D(\bar{v})$, the string-stability condition is described by the following inequality [26]:

$$T_{\mathrm{des}} \geq \frac{-k_2 + \sqrt{{k_2}^2 + 2k_1}}{k_1}. \tag{3.3}$$

3.3 Numerical simulations without JAD

3.3.1 Settings

First, we describe the scenario used for numerical simulations without JAD: 1000 cars labeled $i = 1, \ldots, 1000$ from the head car to the tail car move in a uniform platoon in a single-lane road of infinite length, as shown in Fig. 3.1. Although we use a finite number of cars in the simulations, we assume that many cars run in columns in front of car 1 and behind car 1000. At time $t = 0$, all the cars move at the same velocity v_{MAX} and have the same gap $D(v_{\mathrm{MAX}})\, h_{\mathrm{buf}} = (d + T_{\mathrm{des}} v_{\mathrm{MAX}})\, h_{\mathrm{buf}}$, which is greater than the desired gap $D(v_{\mathrm{MAX}})$. Here, h_{buf} denotes the degree of gap extension compared to $D(v_{\mathrm{MAX}})$ and is set to $h_{\mathrm{buf}} \geq 1$. Because of the restriction $v \leq v_{\mathrm{MAX}}$, once the gap is set, cars $2, \ldots, 1000$ keep the gap $D(v_{\mathrm{MAX}})\, h_{\mathrm{buf}}$. This preservation of the extended gap reflects the behavior in real highway traffic: cars that do not continually keep the desired headway D_i that is uniquely

determined by their velocity [Eq. (3.2)]. Instead, they maintain a gap greater than D_i in a situation where traffic uncongested. Here we emphasize the difference between T_{des} and h_{buf} as follows. T_{des} is an internal parameter in the Helly model that determines the value of the desired gap. On the other hand, h_{buf} is a parameter of initial conditions independent of traffic models, which indicates the degree of gap extension compared to the desired gap. The extended initial gap is expected to cause the dependence of the magnitude of perturbations for the stability of the platoon's flow. If h_{buf} is set to 1, the stability against perturbations is given by Eq. (3.3) regardless of the magnitude of perturbations. In contrast, if h_{buf} is set to be larger than 1, the stability depends on the magnitude of perturbations. In this case, the quantitative discussion of the stability will need numerical simulations (but see [49]). It should be noted that we use h_{buf} because h_{buf} is closely related to the occurrence of the secondary traffic jams of JAD which are discussed later. If h_{buf} is large enough to be stable against the perturbation caused by the absorbing car, this perturbation does not grow to be a secondary jam.

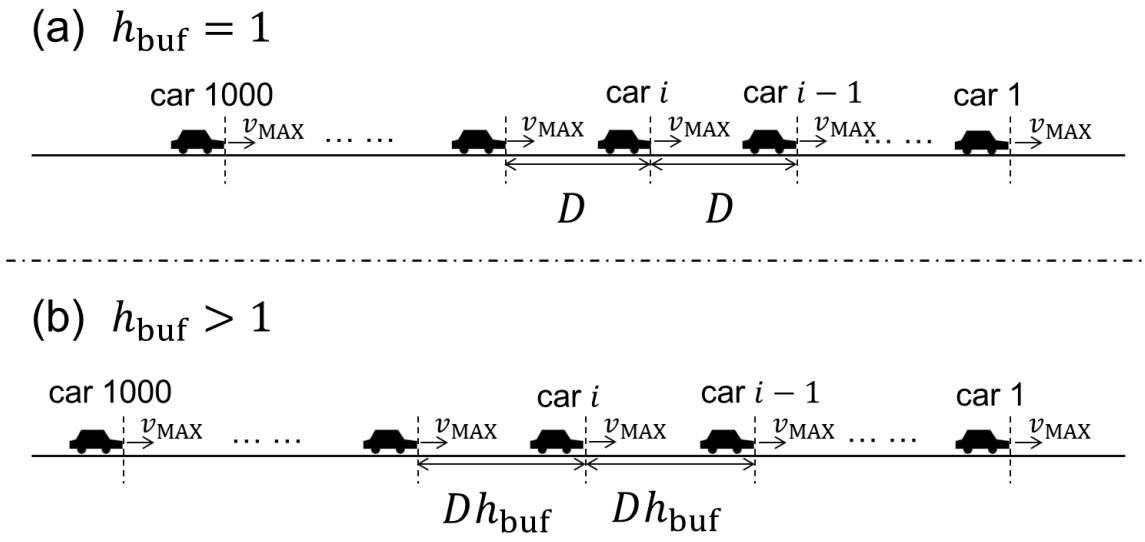

Fig. 3.1. Uniform flow states with velocity v_{MAX} at the beginning of scenario. (a) $h_{\mathrm{buf}} = 1$. (b) $h_{\mathrm{buf}} > 1$. When $h_{\mathrm{buf}} > 1$, although each car's gap is greater than the desired gap $D(v_{\mathrm{MAX}})$, cars maintain v_{MAX} because of the restriction that $v \leq v_{\mathrm{MAX}}$.

We assume that at time $t = t_{S_1}$, car 1 is captured by a perturbation propagating from the downstream area. At that time, it starts to decelerate from v_{MAX} to v_{p} with a constant acceleration $-\alpha_{\mathrm{p}}$. After its velocity reaches v_{p}, it remains at v_{p} for the interval T_{p}. Next, it starts to exit the perturbation and accelerates from v_{p} to v_{MAX} with the acceleration

$\alpha_{\rm p}$. Subsequently, it maintains the velocity $v_{\rm MAX}$. This motion of car 1 is a perturbation in itself and propagates toward the following cars $2, \ldots, 1000$ as per the Helly model with the velocity limit $0 \leq v \leq v_{\rm MAX}$. We set $T_{\rm p} = 10$ [s], $v_{\rm p} = 15$ [m/s], $\alpha_{\rm p} = 0.4$ [m/s^2], $t_{S_1} = 20$ [s], and $v_{\rm MAX} = 25$ [m/s]. The value of $v_{\rm MAX}$ is the maximum highway speed. The parameters of the Helly model are set to $k_1 = 0.2$ [s^{-2}], $k_2 = 0.6$ [s^{-1}], $T_{\rm des} = 1.0$ [s], and $d = 7.5$ [m]. We set $T_{\rm des}$ according to the distribution of netto time gaps for cars found in empirical data from highway traffic [45]. Note that, although Fig. 2 of Ref. [45] reports that the typical peaking netto time gaps varies from roughly 0.7 to 1.5 [s], for simplicity we choose a value within this range and keep it fixed throughout the simulations. The range 7 [m] $\leq d \leq$ 7.5 [m] is often used in physics [19, 37, 50]. String stability in uniform flow with the desired gap, which is a criterion for stability against perturbations [Eq. (3.3)], remains unattained with these parameters. Thus, for $h_{\rm buf} = 1$, a car's braking is amplified and finally the flow is converted into a traffic jam.

The behavior of cars $2, \ldots, 1000$ is calculated with the fourth-order Runge-Kutta method. One time step of the calculation is approximately 0.001 [s]. In one scenario, this calculation is conducted for 3000 [s]. This numerical scheme is also used for other numerical simulations which are explained later.

3.3.2 Results

The time-space diagrams in Fig. 3.2 show the numerically obtained trajectories of cars for $h_{\rm buf} = 1, 1.03, 1.06, 1.09$, and 1.15. The perturbation caused by car 1 grows into a traffic jam for $h_{\rm buf} = 1, 1.03, 1.06$, and 1.09 and decays for $h_{\rm buf} = 1.15$. The velocities at the front and end of the traffic jam are -14.66 [km/h] and -12.40 [km/h] for $h_{\rm buf} = 1$, -8.84 [km/h] and -8.17 [km/h] for $h_{\rm buf} = 1.03$, -7.64 [km/h] and -6.97 [km/h] for $h_{\rm buf} = 1.06$, and -7.02 [km/h] and -6.60 [km/h] for $h_{\rm buf} = 1.09$. To investigate the magnitude of traffic jams, we show the period of the tail car (car 1000) in the stopped state in Table 3.1. The period becomes smaller as $h_{\rm buf}$ becomes larger. The dependence of traffic jam development on $h_{\rm buf}$ results from each car having an extra gap $(h_{\rm buf} - 1)D(v_{\rm MAX})$ to mitigate the perturbation.

3.3.3 Criterion for determining the development of a traffic jam

If the perturbation caused by car 1 is sufficiently amplified, it is expected that a car located far upstream of car 1, such as car 1000, will be stopped by the perturbation.

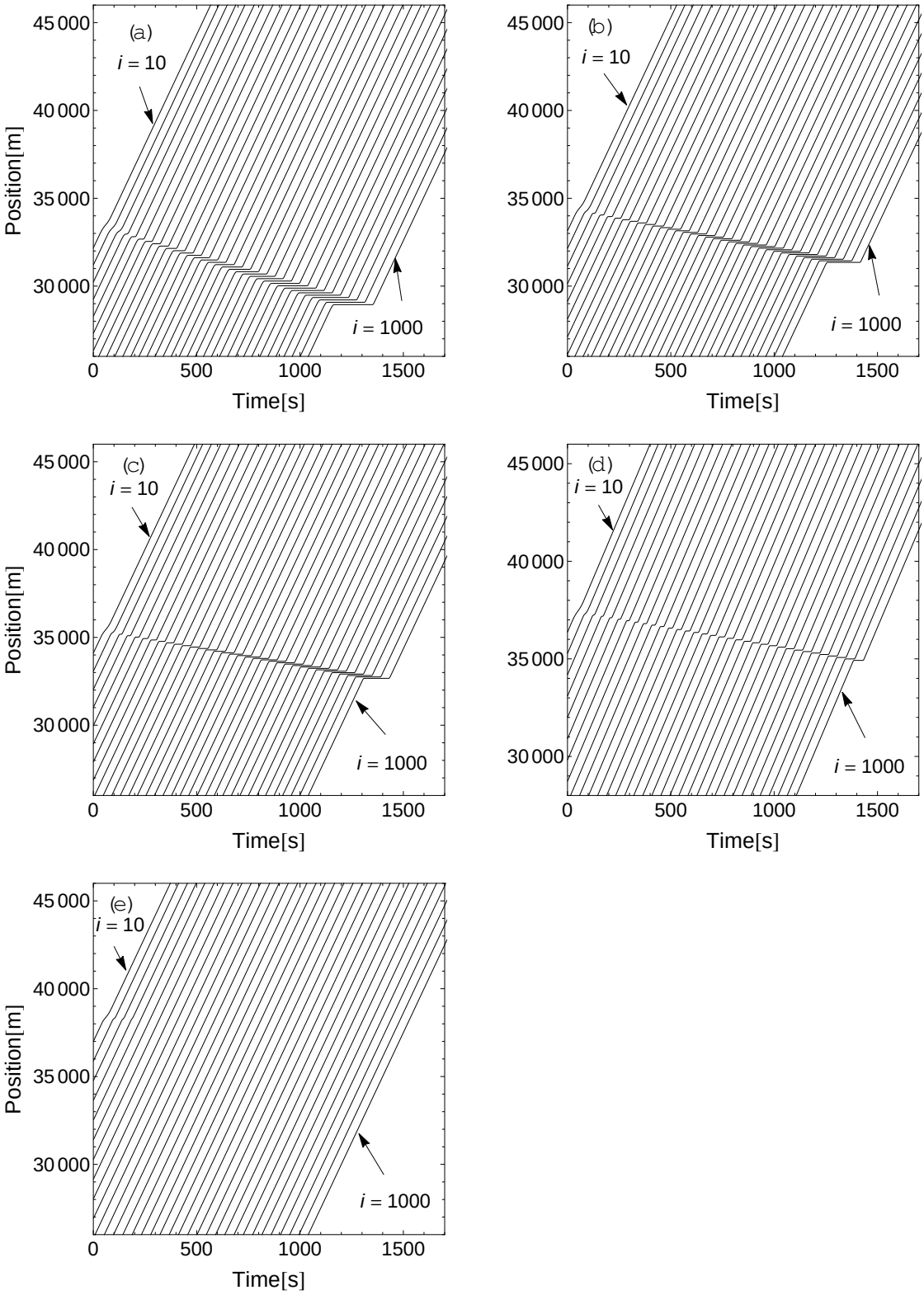

Fig. 3.2. Time-space diagrams without JAD. (a) $h_{\mathrm{buf}} = 1$. (b) $h_{\mathrm{buf}} = 1.03$. (c) $h_{\mathrm{buf}} = 1.06$. (d)$h_{\mathrm{buf}} = 1.09$. (e) $h_{\mathrm{buf}} = 1.15$. The horizontal and vertical axes correspond to time and position, respectively. Each line represents the trajectory of each car. The spatial origin is defined as the position of car 1000 at $t = 0$. The trajectories of every 30 cars from car 10 to car 1000 are shown.

h_{buf}	period for which $v_{1000} = 0$ [s]
1	182.8
1.03	153.7
1.06	116.8
1.09	79.0
1.15	—

Table. 3.1. List of periods for which velocity of tail car of column (car 1000) equals zero. The periods represent the magnitude of the traffic jam.

Thus, the condition whereby the car-1 perturbation grows to become a jam is given by the following criterion:

$$\min_{0<t<3000} v_{1000}(t) = 0. \tag{3.4}$$

On the basis of this criterion, we investigate the v_{p}–T_{p} parameter space where car 1 perturbation is sufficiently amplified to cause a traffic jam. Where the perturbation grows to form a traffic jam [i.e., where Eq. (3.4) is satisfied] is called the "*perturbation growth (PG)*" region and where the perturbation does not grow or decays [i.e., Eq. (3.4) is not satisfied] is called the "*perturbation decay (PD)*" region.

Figure 3.3 shows the boundary between PG and PD in a v_{p}–T_{p} diagram for $h_{\mathrm{buf}} = 1.03$, 1.06, and 1.09. All values except for v_{p}, T_{p}, and h_{buf} are the same as for Fig. 3.2. We determine the boundary lines by binary searches. PG is the region to the left of the boundary and PD is the region to the right of the boundary for each h_{buf}. The quantity T_{p} increases with v_{p} on each boundary because the perturbation is large for small v_{p} and large T_{p}. The PG region is small for large h_{buf}.

3.4 Numerical simulations with JAD

Consider the situation in which the absorbing car performs JAD. The initial condition and the movement of the leading car are the same as in the scenario without JAD. Cars $2, \ldots, m-1, m+1, \ldots, 1000$ obey the Helly model with the restriction $0 \leq v \leq v_{\mathrm{MAX}}$. Car m is the absorbing car and its movement is described as follows: At $t = t_{S_1}$, when the leading car starts to perturb traffic, car m starts to decelerate from v_{MAX} to v_{a} with a constant acceleration $-\alpha_{\mathrm{a}}$. After reaching v_{a}, it maintains v_{a} for a period T_{a}. The absorbing car attempts to avoid the traffic jam by this deceleration (slow-in). Then, it accelerates with a constant acceleration α_{a} from v_{a} to v_{MAX} (fast-out). Subsequently, it

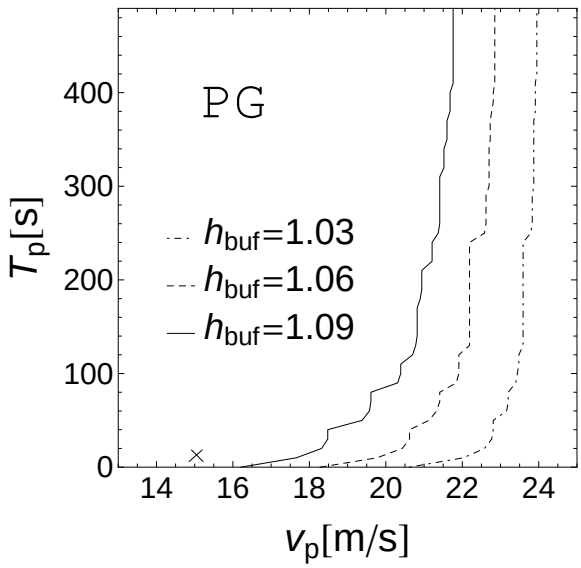

Fig. 3.3. Perturbation growth (PG) and perturbation decay (PD) in a v_{p}-T_{p} diagram. Each boundary line is numerically determined by the condition [Eq. (3.4)] with binary searches. PG and PD are in the left and right side of each boundary, respectively. The cross corresponds to the point (15, 10) as the parameters of the perturbation caused by car 1 in the scenarios with and without JAD.

again follows car $m-1$ with velocity v_{MAX}.

3.4.1 Settings of v_{a} and T_{a}

The parameters v_{a} and T_{a} must satisfy the condition that the absorbing car's velocity should be v_{MAX} and its gap should be the initial gap $D\left(v_{\mathrm{MAX}}\right) h_{\mathrm{buf}}$, when car $m-1$ exits a traffic jam with the maximum velocity v_{MAX}. We express this condition by introducing the two distances Δ_i and Δ_{a} as shown in Fig. 3.4. The distance Δ_i is defined as the loss of the travel distance of car i caused by the leading car's perturbation in the absence of JAD. It is the difference between the actual position $x_i\left(t_{G_i}\right)$ and a virtual position $x_i^I\left(t_{G_i}\right)$. The time t_{G_i} is defined to be the moment when car i attains the velocity v_{MAX}. The imaginary position $x_i^I\left(t\right)$ is defined as the position of car i at time t assuming that it keeps v_{MAX} from time 0 to t. The distance Δ_{a} is defined as the decrease in the absorbing car's travel distance caused by JAD. It is the difference between the actual position $x_m\left(t_{G_m}\right)$ and the imaginary position $x_m^I\left(t_{G_m}\right)$, where car m is designated as the absorbing car. The distance Δ_{a} is given as

$$\Delta_{\mathrm{a}} = \frac{\left(v_{\mathrm{MAX}} - v_{\mathrm{a}}\right)^2}{\alpha_{\mathrm{a}}} + \left(v_{\mathrm{MAX}} - v_{\mathrm{a}}\right) T_{\mathrm{a}}. \tag{3.5}$$

The criteria that $T_{\rm a}$ and $v_{\rm a}$ must satisfy comes from the following equations:

$$\Delta_{m-1} = \Delta_{\rm a}, \tag{3.6}$$

where Δ_{m-1} is determined by numerical simulations. Thus, we obtain

$$T_{\rm a} = \frac{\Delta_{m-1}}{v_{\rm MAX} - v_{\rm a}} - \frac{v_{\rm MAX} - v_{\rm a}}{\alpha_{\rm a}}. \tag{3.7}$$

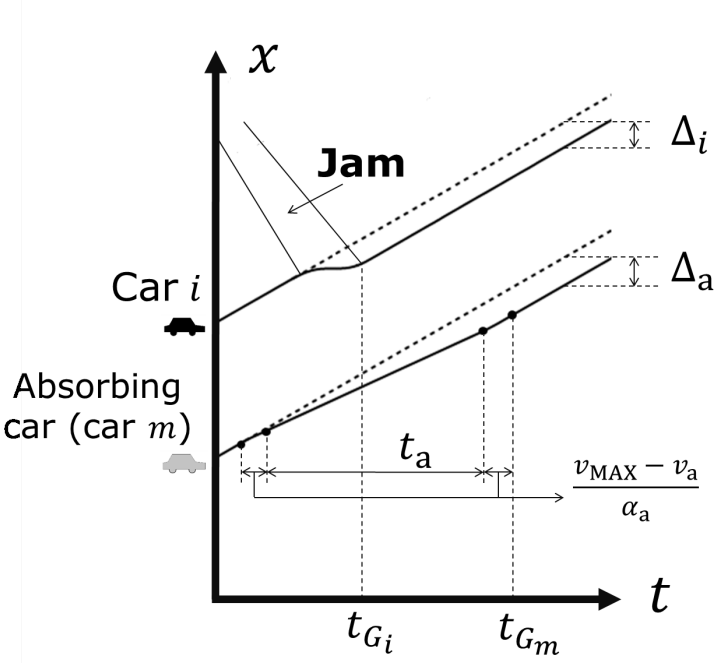

Fig. 3.4. Time-space diagram showing Δ_i and $\Delta_{\rm a}$. Thick broken lines represent the movements of cars i and m if the leading car's perturbation is absent and car m does not perform JAD. The thick solid lines represent the movements of cars i and m if the leading car's perturbation is present and car m performs JAD. Δ_i is the difference between the positions of the thick broken line and the thick solid line at time t_{G_i}. The distance $\Delta_{\rm a}$ is the difference between positions shown by the thick broken line and the thick solid line at time t_{G_m}.

We set $\alpha_{\rm a} = 0.4$ [m/s^2] and $h_{\rm buf} = 1.03, 1.06$, and 1.09 to obtain Δ_{m-1} for $m = 2, \ldots, 1000$. Other values are the same as those in Fig. 3.2. By using the measured values of Δ_{m-1}, we get $T_{\rm a}$ as a function of $v_{\rm a}$, as shown in Fig. 3.5. This relationship gives a reasonable set of ($T_{\rm a}$, $v_{\rm a}$) when performing JAD. We show only $T_{\rm a}$ for $m \geq 100$ because Δ_{m-1} for extremely small m (i.e., when the absorbing car is extremely close to car 1) is qualitatively different from Δ_{m-1} for larger m (see appendix for a detailed discussion).

The quantity $T_{\rm a}$ monotonically increases with $v_{\rm a}$ and sharply increases at nearby

$v_{\mathrm{MAX}} = 25$ [m/s]. This monotonic increase arises because of the long time taken to exit a traffic jam if v_{a} is close to v_{MAX}. The quantity T_{a} increases with m because the traffic jam grows as it propagates upstream. T_{a} decreases as h_{buf} increases because the traffic jam growth rate decreases as the initial gap increases.

3.4.2 Conditions for secondary traffic jam in JAD

The manner in which the absorbing car drives causes compression and expansion waves in the following cars. For a successful JAD, these waves should not grow into a secondary traffic jam. A secondary traffic jam is caused by the absorbing car (car m) if the velocity of an imaginary car $m + 999$, which is behind the tail car (car 1000), approaches zero as a result of the action of the absorbing car (car m). Otherwise, no secondary traffic jam results. To depict the boundary of the secondary traffic jam in a v_{a}-T_{a} diagram, we focus on the motions of the absorbing car and car 1. Their motions are identical: braking with fixed acceleration (α_{a} or α_{p}) from the maximum velocity v_{MAX} to a lower velocity (v_{a} or v_{p}), maintaining the low velocity for a time (T_{a} or T_{p}), and then accelerating at a fixed rate back to the maximum velocity. Therefore, if $\alpha_{\mathrm{a}} = \alpha_{\mathrm{p}}$, the threshold for the occurrence of the secondary traffic jam in a v_{a}-T_{a} diagram is identical to the threshold for the occurrence of the traffic jam caused by car 1 in a v_{p}-T_{p} diagram (Fig. 3.3). The threshold for the occurrence of the secondary traffic jam are depicted in v_{a}-T_{a} planes, as shown in Fig. 3.5. We set $\alpha_{\mathrm{a}} = \alpha_{\mathrm{p}} = 0.4$ [m/s^2] and $h_{\mathrm{buf}} = 1.03$, 1.06, and 1.09. Other values are same as for Fig. 3.2. The left side of each boundary is where the secondary traffic jam occurs and the right side of each boundary is where no secondary traffic jam occurs. JAD can be performed without causing a secondary traffic jam with the values of v_{a} and T_{a} on the lines of Eq. (3.7), which is on the right side of the boundary. As h_{buf} increases, the region where JAD is successful increases.

3.4.3 Restricting JAD starting time

Because the absorbing car has to obtain information about the traffic jam, it cannot start JAD when there is no traffic jam. In other words, it is only able to start JAD after car 1 starts braking. Note that we assume that the perturbation is not observed by the absorbing car when it propagates through the cars preceding car 1. This restriction is

given by

$$T_{\rm a} + 2\frac{v_{\rm MAX} - v_{\rm a}}{\alpha_{\rm a}} \leq t_{G_{m-1}} - t_{S_1}, \tag{3.8}$$

where the left side of this inequality is the JAD period, which spans from the time at which deceleration begins to the time at which acceleration finishes. Here, $t_{G_{m-1}}$ is the time at which car $m-1$ exits the traffic jam and is calculated by numerical simulations. The time t_{S_1} is when the leading car starts causing a perturbation. The boundaries defined by the inequality (3.8) in the $v_{\rm a}$-$T_{\rm a}$ plane are shown by the thick black lines in Fig. 3.5. We set $\alpha_{\rm a} = 0.4$ [m/s^2] and $h_{\rm buf} = 1.03$, 1.06, and 1.09. Other values are the same as Fig. 3.2. The left side of each thick black line corresponds to the region where the restriction is satisfied. It is possible to successfully perform JAD on the line defined by Eq. (3.7) in the region sandwiched between the thick line on the right boundary and the boundary of the secondary traffic jam on the left. When $h_{\rm buf} = 1.03$, the thick line is plotted in the region where secondary jams occur. Thus, it is impossible to perform JAD for any m (≥ 100) without causing a secondary traffic jam. When $h_{\rm buf} = 1.06$, JAD succeeds in a narrow region in the $v_{\rm a}$–$T_{\rm a}$ plane. When $h_{\rm buf} = 1.09$, the region in which JAD succeeds in the $v_{\rm a}$-$T_{\rm a}$ plane is larger than for $h_{\rm buf} = 1.06$.

3.4.4 Examples of success and failure in JAD

We set $h_{\rm buf} = 1.09$, $\alpha_{\rm a} = 0.4$ [m/s^2], $m = 300$, and $v_{\rm a} = 20$ [m/s] and 22 [m/s]. Other values are the same as those in Fig. 3.2. The values of $T_{\rm a}$ are calculated to be 236.9 [s] for $v_{\rm a} = 22$ [m/s] and 129.3 [s] for $v_{\rm a} = 20$ [m/s]. Figure 3.6 show numerically obtained trajectories of cars in time-space diagrams. For $v_{\rm a} = 22$ [m/s] [Fig. 3.6(a)], car 1 starts braking at $t = t_{S_1}$. This perturbation grows to a traffic jam that propagates to car $m-1$. The thick line corresponds to the trajectory of the absorbing car (car m). The absorbing car starts JAD at $t = t_{S_1}$ and enlarges its headway by maintaining its velocity at $v_{\rm a} = 22$ [m/s]. Because of the extended gap, the absorbing car avoids being involved in the traffic jam. The compression and expansion waves caused by the absorbing car decay and finally disappear. However, in the diagram for $v_{\rm a} = 20$ [m/s], the compression wave grows to become a traffic jam [Fig. 3.6(b)].

We plot the point ($v_{\rm a}$,$T_{\rm a}$) = (22, 236.9) in the $v_{\rm a}$-$T_{\rm a}$ plane as a circle and $(v_{\rm a}, T_{\rm a}) = (20, 129.3)$ as a triangle, as shown in Fig 3.5(c). We also mark the point ($v_{\rm p}$, $T_{\rm p}$) with a cross in Fig 3.3. The cross is inside the region where traffic jams occur, which agrees with

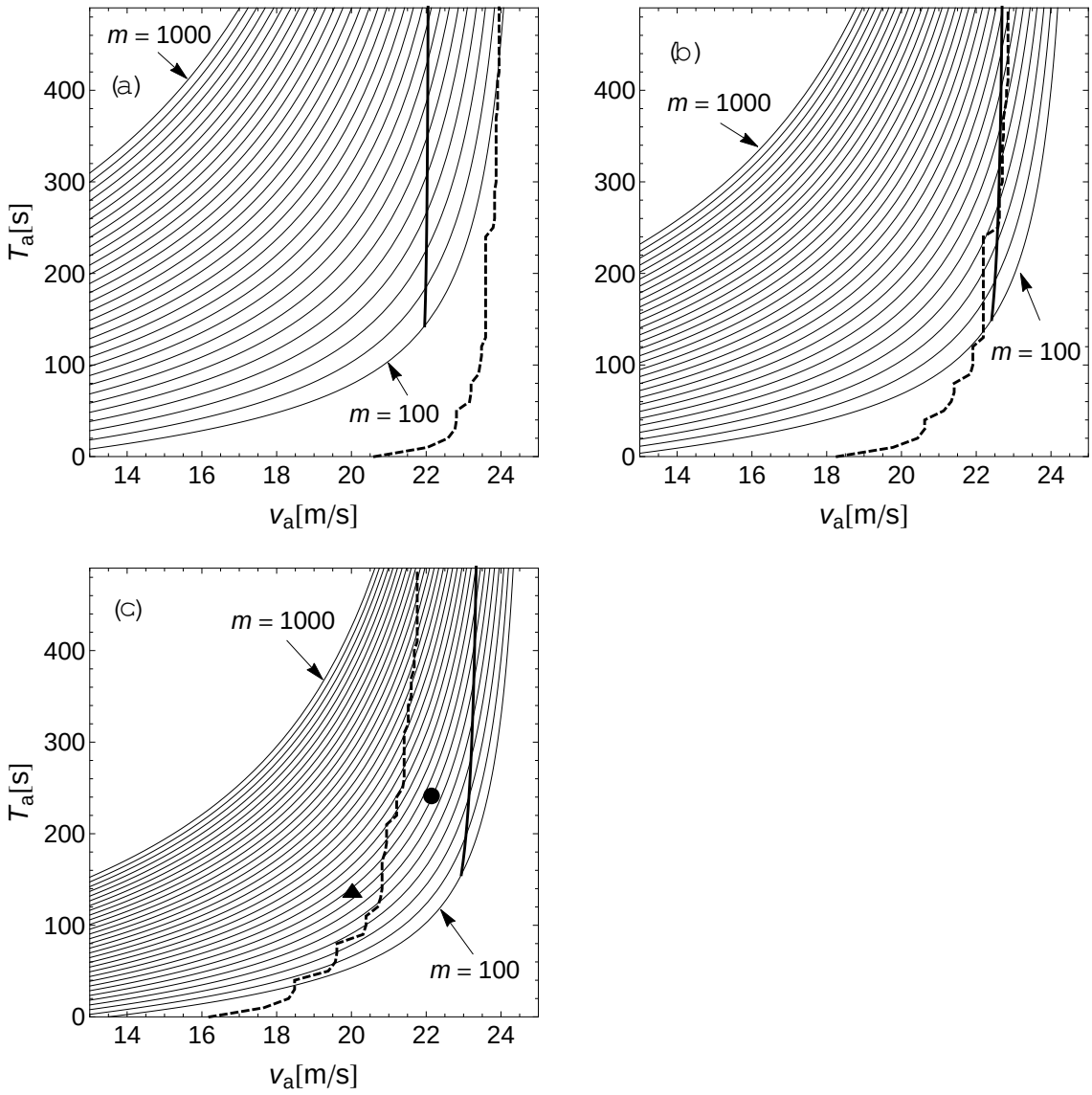

Fig. 3.5. Regions of successful JAD in v_{a}-T_{a} diagrams. (a) $h_{\mathrm{buf}} = 1.03$. (b) $h_{\mathrm{buf}} = 1.06$. (c) $h_{\mathrm{buf}} = 1.09$. The thin black lines represent Eq. (3.7) from $m = 100$ to $m = 1000$ in steps of 30. The thresholds for the occurrence of secondary traffic jams are depicted by broken black lines. The boundaries of the restriction of the starting time for JAD are depicted as thick black lines. They are obtained by connecting the points $(v_{\mathrm{a}}, T_{\mathrm{a}})$ that satisfy the simultaneous equations Eq. (3.7) and $T_{\mathrm{a}} + 2\frac{v_{\mathrm{MAX}} - v_{\mathrm{a}}}{\alpha_{\mathrm{a}}} = t_{G_{m-1}} - t_{S_1}$ for m from 100 to 1000 in steps of 10. JAD succeeds in the v_{a}–T_{a} region on the line of Eq. (3.7) sandwiched between the boundary of the secondary traffic jam on the left and the boundary of the JAD starting-time restriction on the right. The circle and triangle in panel (c) correspond to the point $(v_{\mathrm{a}}, T_{\mathrm{a}}) = (22, 236.9)$ in the case of successful JAD and $(v_{\mathrm{a}}, T_{\mathrm{a}}) = (20, 129.3)$ in the case of the failure of JAD, respectively.

the occurrence of the traffic jam caused by car 1, as shown in Fig. 3.6. The perturbation situated at (v_{p},T_{p}) is removed by JAD and a new perturbation occurs at (v_{a},T_{a}). The circle is in the region where no secondary traffic jam occurs, which agrees with the no secondary traffic jam being observed in Fig. 3.6(a). However, the triangle is in the region where a secondary traffic jam occurs, which agrees with the occurrence of a secondary traffic jam in Fig. 3.6(b).

3.5 Discussion

We developed a JAD with car-following behaviors to represent accelerations of cars and the stability of traffic flows. We investigated relationships between the growth of the perturbations caused by the leading car and an extra amount of initial gap. In addition, we formalized the relationships between the absorbing car's low velocity v_{a} during JAD and the duration T_{a} during which the low velocity is maintained. We integrated the condition for which no secondary traffic jam is caused by JAD with various increases in the initial gap. Moreover, we investigated the restriction imposed by the starting time for JAD. By combining these conditions, we verified the existence of a region in the v_{a}-T_{a} plane where JAD succeeds in avoiding a traffic jam. Furthermore, we numerically confirmed the accuracy of our classification of the regions of parameter space into regions of success and failure for JAD. Finally, we demonstrate that JAD is robust against α_{a} (see B.2) and robust against the choice of car-following models through investigations with the intelligent driver model (IDM) [46, 50] (see B.3).

We found that the region of success for JAD in the v_{a}-T_{a} plane increases as h_{buf} increases. In real highway traffic, in the region far upstream of a traffic jam, the traffic density is expected to be lower than in the region of the traffic jam. Therefore, JAD should be started far upstream of a traffic jam.

According to the kinematic theory in Ref. [44], JAD does not cause a secondary traffic jam if the traffic density upstream of a traffic jam is lower than a critical density. Our study indicates a richer phenomenon whereby, even if cars have an extra gap, there exists the case where a secondary traffic jam occurs by JAD. This phenomenon is because of the introduction of car-following behavior and to the treatment of the growth and decay of perturbations into JAD.

Regarding the influence of JAD on the capacity of bottlenecks [51], we would like to emphasize that JAD does not reduce the capacity of bottlenecks. This is because JAD is

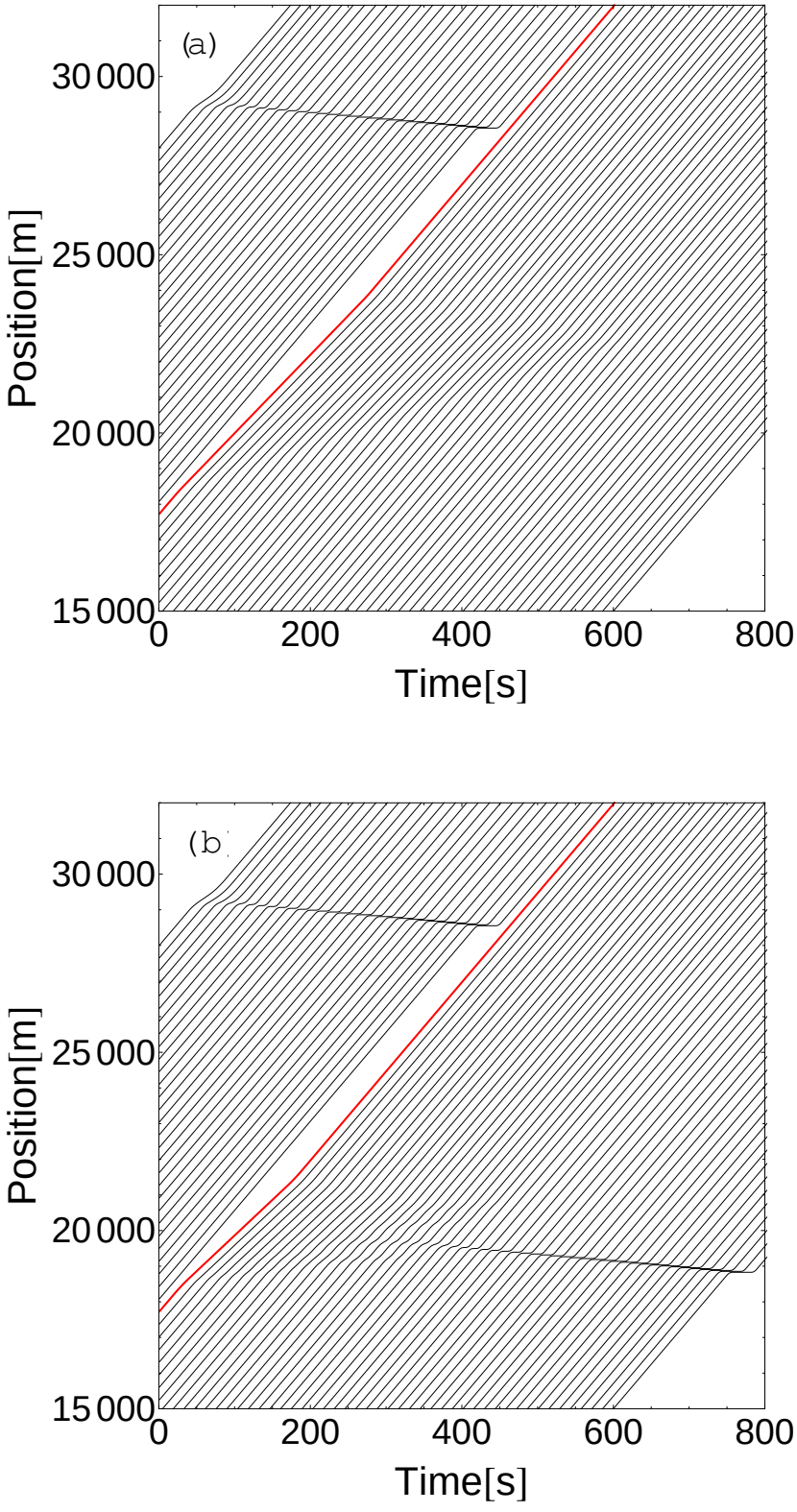

Fig. 3.6. Time–space diagrams for JAD. (a) Success with $v_a = 22$ [m/s]. (b) Failure with $v_a = 20$ [m/s] because of the occurrence of a secondary traffic jam. The thick red lines are trajectories of the absorbing car.

performed in the PD region (see Fig. 3.3). In the PD region, the following cars weaken the perturbation of the absorbing car by consuming their inter-vehicular distances; therefore, the perturbation finally disappears. After the disappearance of the perturbation, the following cars do not have to decelerate nor shorten their headways.

When $h_{\mathrm{buf}} = 1$, the compression wave caused by car 1 propagates at -14.66 [km/h], which is reasonable when compared with real measurements (e.g., -15 [km/h] [52] and roughly -19 feet per second ≈ -21 [km/h] [53]; see Figs. 3.3 and 3.4 of Ref. [53]). However, the velocities for larger h_{buf} are much less. Although it may seem unnatural, in real traffic the propagation velocity is unknown for traffic density below the critical density (i.e., for large h_{buf}). The relationship between the propagation velocity and traffic density will be the focus of future studies.

Explicit relations of parameters for the success of JAD will be helpful for guiding JAD. However, it is difficult to derive them because the stability depends on the magnitude of perturbations. To derive them is our future works.

Chapter 4

Demonstration experiment of JAD

In this chapter, we demonstrate an experiment to observe the effect of JAD in the presence of drivers' reaction delay and the inaccuracy of human driving. The experiment involves five human-driven cars riding in a platoon around a circuit. Perturbations caused by the first car are absorbed by the third car, which prepares a long headway in advance. We investigate the affection of JAD on the traffic flow in the aspect of travel time. Furthermore, the reduced acceleration requirements lead to clear improvements in fuel consumption.

4.1 Description of experiment

4.1.1 Experimental scenario

The experiment involves five cars driving in a column around a circuit. The cars are named car-1, ..., car-5 in order from the leading car and only car-3 is the absorbing car. We assume that a traffic jam has occurred far upstream of them and car-1 and car-2 are eventually caught up in it, by contrast, car-3 attempts to remove it. We define h_i as the sum of car-i' s inter-vehicular distance and its length. All cars are initially stationary with the intervals such that car-2, car-4 and car-5 have $h_i = h_0$ $(i = 2, 4, 5)$ and car-3 has $h_3 = h_{\mathrm{a}}$. All cars are ordered to start simultaneously and run in a platoon at velocity v_{F}. Car-2, car-4, and car-5 are ordered to retain $h_i = h_0$ $(i = 2, 4, 5)$ and car-3 is ordered to retain $h_3 = h_{\mathrm{a}}$. Once a stable platoon is formed, car-1 causes a perturbation by a sequence of actions: decelerating from v_{F} to v_{J}, maintaining v_{J} over period T and accelerating to v_{F}. These actions correspond to the situation in which car-1 enters the jam, is trapped within the jam for time T, and then exits. If h_{a} is insufficiently large,

car-3 and its followers become involved in the perturbation and must brake in turn. If h_{a} is large enough, car-3 removes the perturbation by maintaining v_{F} and decreasing h_3 from h_{a}; thus, the following cars need not brake at all.

Because drivers are situated in a circuit and they are aware that they participate in an experiment, their psychological conditions in our experiment are probably different from those in real traffic. Accordingly, the so-called memory effect, which is observed in real highway traffic, is probably absent in our experiment. This effect is the extension of net time gaps between two successive cars trapped in a jam over a considerably long period [45, 46]. Hence, we assume h_i $(i = 2, \ldots, 5)$ do not extend from h_0 after entangled in the perturbation.

4.1.2 Experimental setup

The circuit is composed of two straight lines and two circular curves, as shown in Fig. 4.2 and in Fig. 4.3. Car-1 was ordered to drive at $v_{\mathrm{F}} = 9.72$ [m/s] (35 [km/h]). The points A and B, where car-1 induced the perturbation, are shown in Fig. 4.2. At Point A, the car was ordered to decelerate to $v_{\mathrm{J}} = 5.56$ [m/s] (20 km/h) and maintain this velocity. At Point B, it was ordered to accelerate to v_{F}. The period over which car-1 drives at v_{J} was set to $T = 15$ [s], and the interval between A and B was set to $v_{\mathrm{J}}T = 83.3$ [m]. The initial h was set to $h_1 = 13$ [m]. The effect of the action of car-3 on the following cars was investigated at different h_{a}. We show typical two examples of h_{aI} in Fig. 4.2.

It should be noted that values of v_{F}, v_{J} and T are fixed throughout all trials. This fixed setting is due to the effect of learning of drivers, which largely affects the result. If the number of trials were increased, drivers would be likely to learn the braking point (deceleration point) of car-1 and thus maintain a greater distance before braking. It should be also noted that car-5 does not come into the sight of car-1 during our experiment.

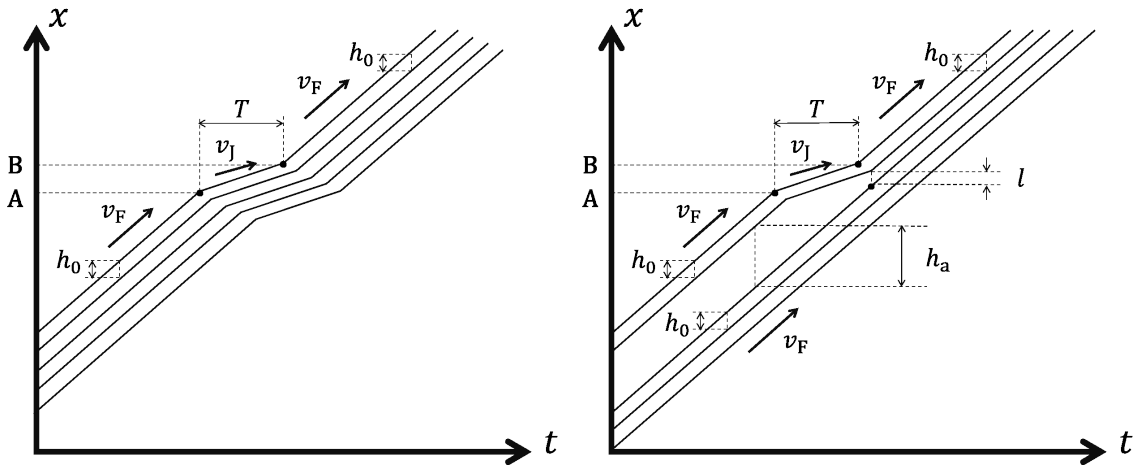

Fig. 4.1. Time-space diagrams of the kinematic-like model for two initial gaps of car-3: (Left) $h_a = h_0$ and (Right) $h_a = l + (v_F - v_J)T$. In the left panel, cars move in the positive x direction (denoting upstream to downstream) in a homogeneous platoon at velocity $v = v_F$ with gap $h_i = h_0$ $(i = 2, \ldots, 5)$. Points "A" and "B" correspond to the deceleration and acceleration points, respectively, mentioned in Sec. 4.1.2. Once the second and succeeding cars encounter the perturbation caused by car-1, they decelerate to $v = v_J$. After running at $v = v_J$ for time T, the velocity of car-1 alters to $v = v_F$, then the gaps of the following cars return to $h_i = h_0$ $(i = 2, \ldots, 5)$ in turn. It should be noted that we do not assume the memory effect [45, 46] in our experiment. In the right panel, the long gap of car-3 buffers it from the perturbation. Thus, car-3 and its followers do not need to brake at all.

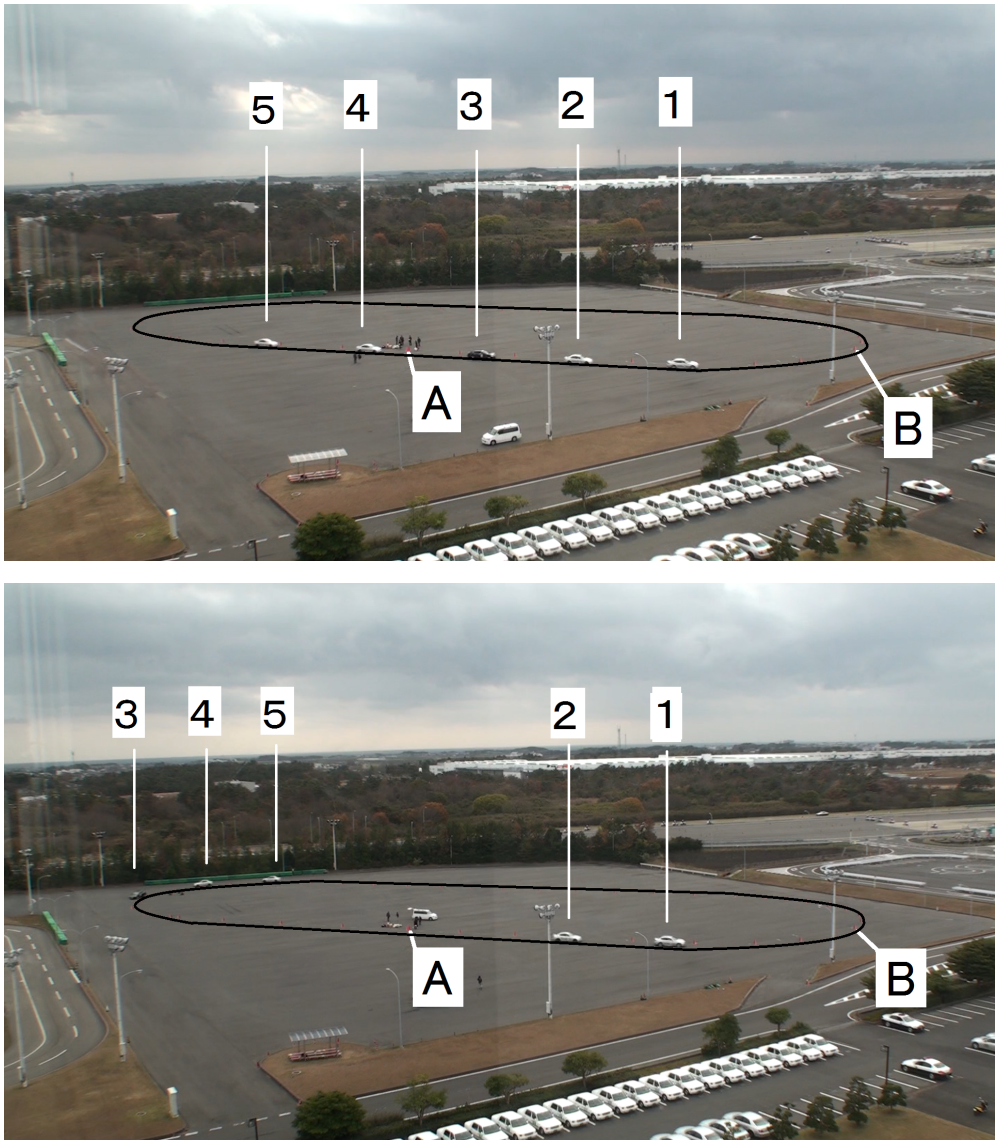

Fig. 4.2. Overhead view of the experimental setup for different h_{a}. Five cars run counterclockwise around the circuit. As a visual guide, the circuit is delineated by black lines. Points "A" and "B" correspond to the deceleration and acceleration points, respectively. The black car (car-3) is the absorbing car. The initial settings of car-3 are given as (Top) $h_{\mathrm{aI}} = 13$ [m] and (Middle) $h_{\mathrm{aI}} = 80$ [m].

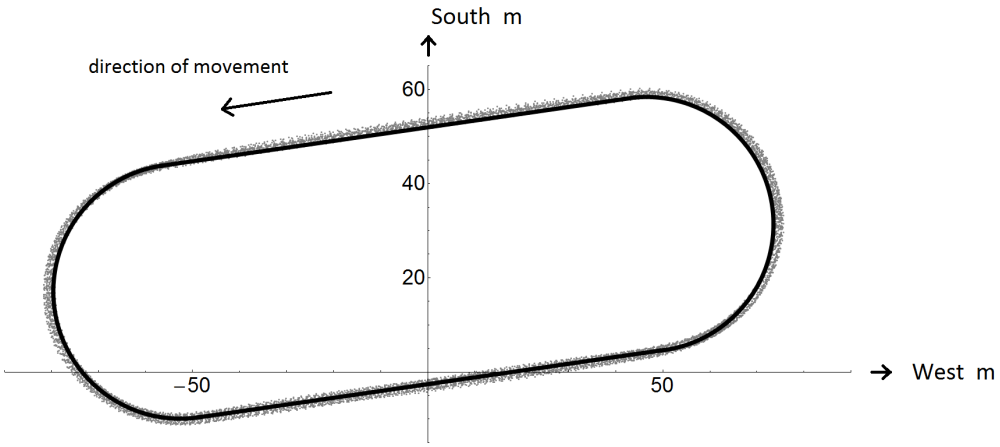

Fig. 4.3. The circuit track (black line) together with a car's trajectory during a test run before the experiment (gray dots). The car completed seven laps. The horizontal and vertical axes denote the longitude (positive direction is West) and latitude (positive direction is South), respectively.

4.2 Experimental results

Because cars were driven by human drivers, car-3 is not able to keep $h_3 = h_{\mathrm{a}}$. Hence, we distinguish between the setting values and the measured values of h_{a}. We denote h_{aI} as the value of h_3 initially set in the halting state and h_{aM} as the measured value of h_3 immediately before car-1's perturbation. The subscripts I and M denote "initial" and "measured", respectively (The measuring procedure is explained in Fig. 4.4 (a)(b) and Fig. C.1 in appendix C.1.). The relationship of h_{aI} and h_{aM} is shown in Tab. 4.1. Most of h_{aM} are larger than h_{aI} because the absorbing car, which has a larger gap, is likely to start more slowly than other cars at the beginning of the trials.

We conduct 19 trials at various values of h_{aM}. They are categorized into "success" or "failure" based on the minimal velocity of car-3; absorption driving is considered successful if the minimal velocity exceeds $v_{\mathrm{J}} = 5.56$ [m/s] (20 [km/h]). At this velocity, the perturbation generated by car-1 is not amplified when it passes through car-3. The results are also shown in Tab. 4.1. Jam absorption success are likely when $h_{\mathrm{aM}} > 50$ [m]. Clearly, JAD implemented at middle or large h_{aM} absorbs the impact of jamming. Comparing the travel time, defined as the time interval between the passing of car-1 through deceleration point A and the arrival of car-5 at acceleration point B, in the trials $h_{\mathrm{aM}} > 50$ with that in the trials $h_{\mathrm{aM}} < 50$, middle h_{aM} such as around 60 [m] does not worsen the travel time. On the other hand, excessively large h_{aM} such as $h_{\mathrm{aM}} > 80$ worsens the travel time.

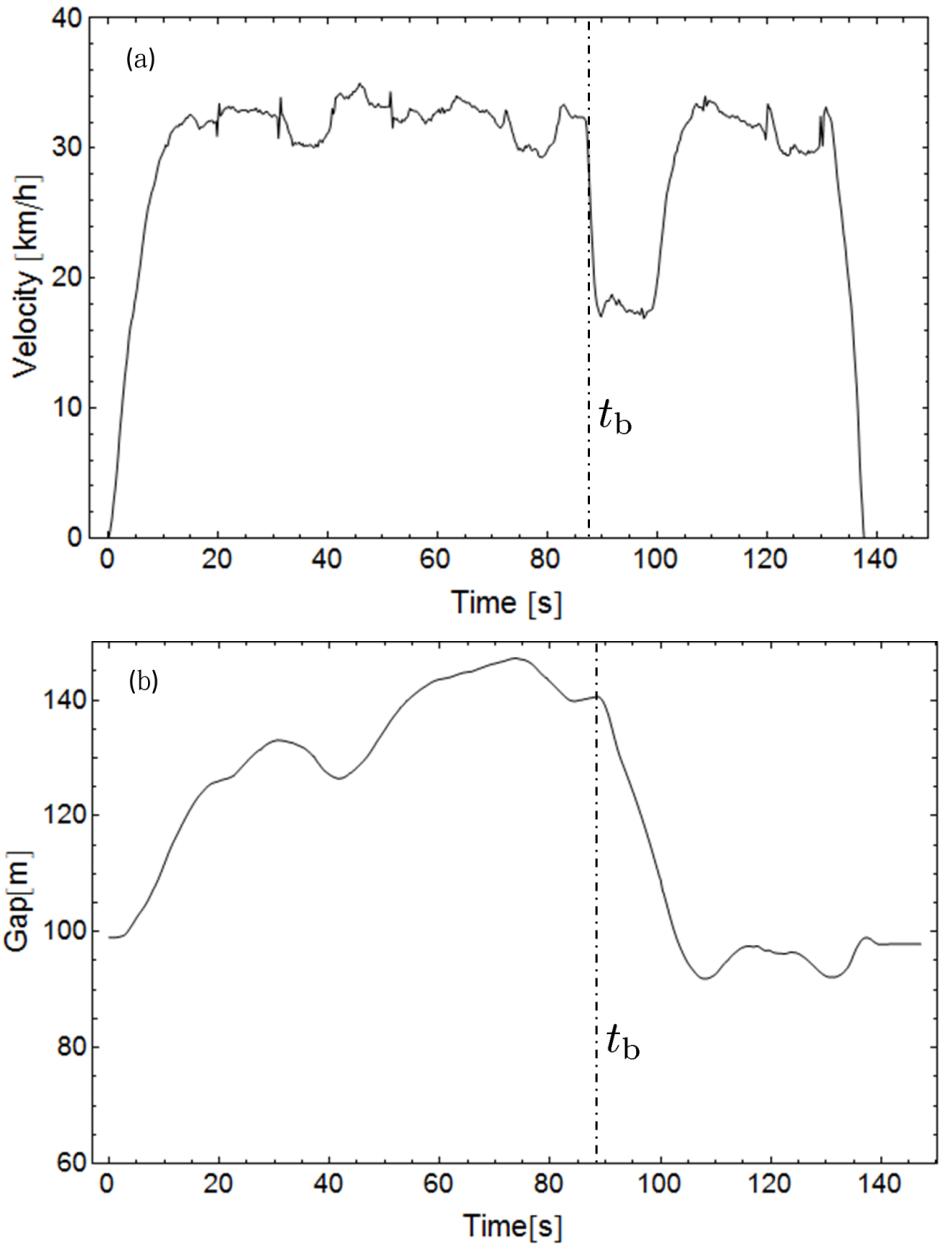

Fig. 4.4. (a) An example of time-velocity diagram of car-1 and (b) time-headway diagram of car-3 from trial 11. To measure h_{aM}, we define t_b as the time when car-1 begins to brake. In each trial, we measure t_b as the time when the acceleration of car-1 first falls below -1 [m/s^2] (see (a)). h_{aM} is calculated as the averaged gap of the absorbing car (car-3) for 20 [s] immediately before t_b (see (b)).

No.	h_{aI} [m]	h_{aM} [m]	$v_{\min}$ [m/s]	success/failure	travel time [s]
1	13	16.3	3.89	×	25.57
2	13	14.1	4.53	×	23.73
3	13	15.3	4.46	×	24.87
4	13	15.4	4.50	×	24.67
5	13	15.9	4.84	×	23.77
6	13	17.2	4.22	×	23.03
7	13	21.4	4.37	×	25.30
8	13	20.9	5.07	×	25.80
9	13	18.5	4.50	×	24.20
10	13	18.3	4.49	×	24.07
11	100	143.8	8.69	◯	32.63
12	80	120.2	7.65	◯	31.03
13	50	64.1	6.89	◯	24.00
14	50	62.6	7.17	◯	23.57
15	40	71.1	6.50	◯	27.37
16	40	56.4	6.19	◯	23.67
17	40	40.4	4.70	×	23.10
18	40	39.6	3.86	×	25.04
19	35	42.9	3.46	×	24.26

Table. 4.1. Trial number, initial values of the gap of the absorbing car h_{aI}, measured minimal velocity of the absorbing car $v_{\min}$, measured parameter h_{aM}, success or failure of JAD and travel time. The procedure of measuring h_{aM} is described in Fig. 4.4 (a)(b) and its caption. $v_{\min}$ is measured between the start time of car-1's perturbation and the time 10 [s] before the absorbing car stops at the end of a run. In each trial, absorption driving is said to succeed if $v_{\min}$ exceeds 5.56 [m/s] (=20 [km/h]), and to fail otherwise. Success and failure of JAD are denoted by ◯ and ×, respectively.

We next investigate the fuel consumptions of car-4. Data from car-5 are not used in this assessment because car-5 received no rear pressure to accelerate. Figure 4.5 is a bar chart of the specific fuel consumption of car-4 in each of the 19 trials, defined as the ratio of the fuel consumption to that of car-4 in trial 1. When h_{aM} exceeds 50 [m] (corresponding to the trials $11-16$, in which jam reduction succeeded), the fuel consumption is likely to be lower than when h_{aM} is below 50 [m]. This difference arises because the absorbing car's deceleration is small when $h_{\mathrm{aM}} > 50$ [m]. The fuel consumption at $h_{\mathrm{aM}} < 50$ [m] was roughly constant because, under this condition, the absorbing car and its followers were forced to brake and then accelerate. This action consumes approximately the same amount of fuel regardless of inter-vehicle distance.

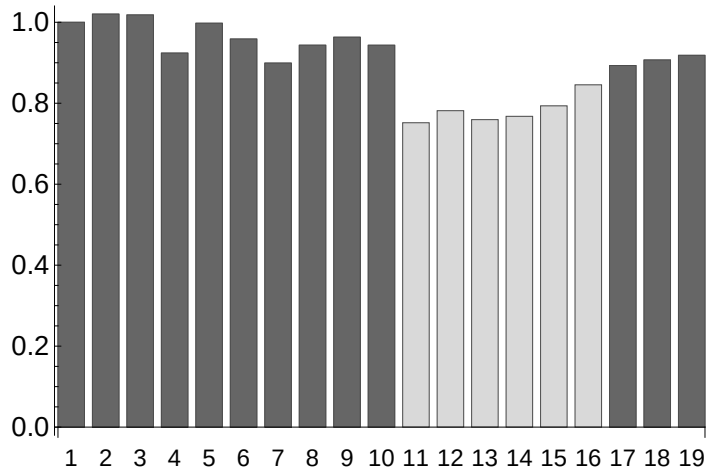

Fig. 4.5. Specific fuel consumptions of car-4, defined as the ratio of the fuel consumption to that of trial 1. The horizontal labels of the chart denote the trial number. Darker and lighter gray bars denote the trials at $h_{\mathrm{aM}} > 50$ [m] and $h_{\mathrm{aM}} < 50$ [m], respectively.

4.3 Discussion

This paper demonstrates the performance of JAD in an experiment involving five human-driven cars around a closed circuit. Car-3 attempted to absorb perturbations caused by car-1 by its initially enlarged space h_{aI}. The experiment neglected the memory effect observed in real highway traffic [45, 46]. If measured value h_{aM} was insufficiently large, the perturbation absorption failed, resulting in larger fuel consumption. On the other hand, excessively large h_{aM} increased the travel time. JAD at middle h_{aM} successfully absorbed the perturbation and maintained an appropriate travel time. In appendix C.1, we calculate the boundary of the headway h_{aM} which distinguishes success and failure of JAD.

In the aspect of saving fuel consumption with microscopic strategies, previous experimental studies reported the improvement of fuel consumption with ACC systems [54, 55]. By contrast, in this paper, we report the improvement only by manually-driven cars.

Because actual traffic demand is controlled in open systems, the experiments should ideally be conducted on a real open highway rather than in a closed system. Nevertheless, changing the initial positions of the cars in a closed system corresponds to controlling specific inflow in an open system. Hence, we believe that it is reasonable to use a closed circuit throughout the experiment.

If two or more absorbing cars exist, we recommend each of them to behave as the sole absorbing car. In this case, the absorbing cars except the first absorbing car cause unnecessary gaps. However, similar to the first absorbing car, the second and succeeding absorbing cars initiate JAD far upstream of the jam, where the traffic density is sufficiently small. Therefore, the unnecessary gaps do not decelerate the cars far upstream. If the absorbing cars catch up with the preceding cars, they should avoid collisions and maintain synchronized movement with those cars.

Lastly, we list future works as follows. We must include the memory effect by performing social JAD experiments in real highway traffic. In our experiment, The travel times in the trials in which the absorption driving is successful are not smaller than those in the trials without absorption driving ($h_{\mathrm{aI}} = 13$ [m]). In real traffic in which drivers are likely to be affected by the memory effect, JAD is expected to improve the travel time by preventing the occurrence of this effect. Because the length of the straight track was limited, our present experiment was conducted at low velocity (around 35 [km/h]). Further investigations of JAD should be conducted at speeds typically reached on Japanese highways, i.e., around 100 [km/h]. In addition, the current experiment tested a simplified JAD with initially enlarged gaps. As the next step, we aim to examine JAD under the consecutive actions of “slow-in” and “fast-out” [44].

Chapter 5

Conclusion

In this paper, we explained the mechanism of the traffic jam and models to reveal the mechanism and have introduced the previous studies for solving traffic jam in chapter 1. As a new solution of the problem, we focused "jam-absorption driving (JAD)" proposed in Ref. [44]. In chapter 2, we described the previous result that JAD is revealed to remove traffic jam with a kinetic model. Then, we conduct the numerical simulations of JAD with the system which represents the dynamical behaviors of cars such as the accelerations and the stability of traffic flow in chapter 3. With the simulation, we explained that JAD has an effect on removing traffic jam. In chapter 4, we conclude that the method of JAD does not worsen the traffic jam under the existence of the fluctuations by human driving. From these findings, we believe JAD valid for solving traffic jam.

There are other strategies to reduce traffic jams. One strategy is to make drivers more reactive and anticipative, which can be achieved by simple local driver-assistance systems such as ACC [26, 36, 37, 39, 40] or driving lessons. Moreover, efficient driving behaviors and location-dependent ACC systems are reported to have robust effects in reducing jams [38, 51]. To conduct JAD together with these other methods would be possible and should be investigated as a future work.

In Ref. [44] and the present study, the absorbing car actively ceases its car-following behavior and then begins again. This active switching off and on of the car-following behavior is different from the studies to improve car-following behaviors with ACC [36–41]. Related to the elimination of jams, Kerner reported that jam growth was disrupted and jams were considerably dissolved by the cars keeping large headways by empirical data and numerical simulations [56]. In the simulations performed in Ref. [56], each car did not intend to remove a jam nor avoid a secondary traffic jam. In contrast, in our study the absorbing car aims to remove the traffic jam and avoid a secondary traffic jam.

In the present study, we assumed that the absorbing car has information about the growth and propagation of the perturbation caused by car 1. The problem of transmitting information on the jam is possibly solved by vehicle-to-vehicle [57, 58] or vehicle-to-infrastructure communications [59], which give the absorbing car the information about the position and velocity of the cars in the downstream direction.

In the future, we believe that JAD will be useful as a function of the automated driving technologies, which has been developed progressively. At the current stage, each automated driving cars aim to move safely by recognizing the surroundings such as the neighbor cars and road signs. As the next stage, automated driving technologies will have been expected to improve the whole traffic flow in a highway. The automated cars can solve the problem by predicting the transmission of jam and automatically moving with v_{a} for t_{a} calculated by method of JAD.

In operating JAD, it is necessary to predict the behaviors of the driver performing JAD and other drivers surrounding it. This prediction is a challenging problem in the current stage. It is also necessary to predict the influence of reactions of other drivers with adverse effects (e.g., changing lanes aggressively and causing jam-stirring disturbances) on the performance of JAD. These adverse effects would impose road conditions on JAD (e.g., single-lane roads where overtaking is banned or roads where overtaking possibility is restricted). Hence the road conditions suitable for JAD should be investigated.

Although the research of JAD is in the primary stage, we believe that it is worth considering and that it will also stimulate other studies related to jam mitigation.

Acknowledgment

I have studied the traffic flow for three years as a doctoral student. I am deeply grateful to Professor Nishinari, the supervisor. During the doctoral course, I have received many generous support from him, for example, the advice for the progress of my study and the chance to collaborate with several motor companies. As my colleague, Nishi, Ezaki, and Tomoeda gave me many constructive comments. Furthermore, every student in Nishinari laboratory helped me when I was in trouble and sometimes did recreation with me. Finally, I would like to thanks my family for mental support and encouragements.

In Chapter 1, the figure 1.1 is permitted to be printed by Tomoeda, who has already used in his doctoral thesis. I also like to express my thanks to him for this permission.

Bibliography

[1] Road Bureau, Ministry of Land, Infrastructure, Transport and Tourism, Japan. `http://www.mlit.go.jp/road/ir/ir-perform/h19/02.pdf`. (accessed 28.03.2016, Japanese).

[2] East Nippon Expressway Company Limited, Japan. `http://www.e-nexco.co.jp/activity/safety/detail_07.html`, 2013. (accessed 28.03.2016, Japanese).

[3] C. F. Daganzo. *Fundamentals of Transportation and Traffic Operations.* Elsevier Science, New York, 1997.

[4] Debashish Chowdhury, Ludger Santen, and Andreas Schadschneider. Statistical physics of vehicular traffic and some related systems. *Physics Reports*, 329(4–6):199–329, 2000.

[5] Dirk Helbing. Traffic and related self-driven many-particle systems. *Review of Modern Physics*, 73(4):1067–1141, 2001.

[6] The Committee on Traffic Flow Theory and Characteristics (AHB45). Traffic flow theory monograph a state-of-the-art report revised 2001. http://www.tft.pdx.edu/docs.htm, 2001.

[7] B. S. Kerner. *The Physics of Traffic: empirical freeway pattern features, engineering applications, and theory.* Springer, Berlin, 2004.

[8] B. S. Kerner. *Introduction to modern traffic flow theory and control: the long road to three-phase traffic theory.* Springer, Berlin, 2009.

[9] Andreas Schadschneider, Debashish Chowdhury, and Katsuhiro Nishinari. *Stochastic Transport in Complex Systems: From Molecules to Vehicles.* Elsevier Science, Amsterdam, 2010.

[10] Mark Brackstone and Mike McDonald. Car-following: a historical review. *Transportation Research Part F*, 2(4):181 – 196, 1999.

[11] Takashi Nagatani. The physics of traffic jams. *Rep. Prog. Phys.*, 65(9):1331, 2002.

[12] Michael J Lighthill and Gerald Beresford Whitham. On kinematic waves. ii. a theory of traffic flow on long crowded roads. *Proceedings of the Royal Society of London.*

Series A. Mathematical and Physical Sciences, 229(1178):317–345, 1955.

[13] Toshimitsu Musha and Hideyo Higuchi. Traffic current fluctuation and the burgers equation. *Japanese Journal of Applied Physics*, 17(5):811–816, 1978.

[14] B. S. Kerner and P. Konhäuser. Structure and parameters of clusters in traffic flow. *Phys. Rev. E*, 50:54–83, Jul 1994.

[15] Dirk Helbing. Improved fluid-dynamic model for vehicular traffic. *Phys. Rev. E*, 51:3164–3169, Apr 1995.

[16] Martin Treiber, Ansgar Hennecke, and Dirk Helbing. Derivation, properties, and simulation of a gas-kinetic-based, nonlocal traffic model. *Phys. Rev. E*, 59:239–253, Jan 1999.

[17] A Aw and Michel Rascle. Resurrection of" second order" models of traffic flow. *SIAM journal on applied mathematics*, 60(3):916–938, 2000.

[18] Raimund Bürger and Kenneth Hvistendahl Karlsen. On a diffusively corrected kinematic-wave traffic flow model with changing road surface conditions. *Mathematical Models and Methods in Applied Sciences*, 13(12):1767–1799, 2003.

[19] Kai Nagel and Michael Schreckenberg. A cellular automaton model for freeway traffic. *Journal de Physique I*, 2(12):2221–2229, 1992.

[20] Marcus Rickert, Kai Nagel, Michael Schreckenberg, and Andreas Latour. Two lane traffic simulations using cellular automata. *Physica A: Statistical Mechanics and its Applications*, 231(4):534–550, 1996.

[21] Elmar Brockfeld, Robert Barlovic, Andreas Schadschneider, and Michael Schreckenberg. Optimizing traffic lights in a cellular automaton model for city traffic. *Phys. Rev. E*, 64:056132, Oct 2001.

[22] Jörg Esser and Michael Schreckenberg. A cellular automaton traffic flow model for online-simulation of urban. In *Cellular Automata: Research Towards Industry: ACRI' 98?Proceedings of the Third Conference on Cellular Automata for Research and Industry, Trieste, 7–9 October 1998*, page 185. Springer Science & Business Media, 2012.

[23] Denos C Gazis, Robert Herman, and Richard W Rothery. Nonlinear follow-the-leader models of traffic flow. *Operations Research*, 9(4):545–567, 1961.

[24] Masako Bando, Katsuya Hasebe, Akihiro Nakayama, Akihiro Shibata, and Yuki Sugiyama. Dynamical model of traffic congestion and numerical simulation. *Physical Review E*, 51:1035–1042, 1995.

[25] W Helly. Simulation of bottlenecks in single-lane traffic flow. *Proceedings of Sympo-*

sium on the traffic flow, pages 207–238, 1959.

[26] Chi ying Liang and Huei Peng. Optimal adaptive cruise control with guaranteed string stability. *Taylor & Francis*, 32, 1999.

[27] Markos Papageorgiou and Apostolos Kotsialos. Freeway ramp metering: an overview. *IEEE Transactions on Intelligent Transportation Systems*, 3(4):271–281, 2002.

[28] M.J. Cassidy and J. Rudjanakanoknad. Increasing the capacity of an isolated merge by metering its on-ramp. *Transportation Research Part B*, 39(10):896–913, 2005.

[29] S. Smulders. Control of freeway traffic flow by variable speed signs. *Transportation Research Part B*, 24(2):111–132, 1990.

[30] E. van den Hoogen and S. Smulders. Control by variable speed signs: results of the dutch experiment. In *7th International Conference on Road Traffic Monitoring and Control*, pages 145–149, London, April 1994. IEEE Conference Publication.

[31] A. Hegyi, B. De Schutter, and J. Hellendoorn. Optimal coordination of variable speed limits to suppress shock waves. *IEEE Transactions on Intelligent Transportation Systems*, 6(1):102–112, 2005.

[32] Hai Yang and Hai-Jun Huang. *Mathematical and economic theory of road pricing.* 2005.

[33] Kenneth A Small and Erik T Verhoef. *The economics of urban transportation.* Routledge, 2007.

[34] David Levinson. Equity effects of road pricing: A review. *Transport Reviews*, 30(1):33–57, 2010.

[35] Ardalan Vahidi and Azim Eskandarian. Research advances in intelligent collision avoidance and adaptive cruise control. *IEEE Transactions on Intelligent Transportation Systems*, 4(3):143–153, 2003.

[36] Martin Treiber and Dirk Helbing. Microsimulations of freeway traffic including control measures. arXiv:cond-mat/0210096, 2002.

[37] L. C. Davis. Effect of adaptive cruise control systems on traffic flow. *Physical Review E*, 69(6):066110, 2004.

[38] Arne Kesting, Martin Treiber, Martin Schönhof, and Dirk Helbing. Adaptive cruise control design for active congestion avoidance. *Transportation Research Part C*, 16(6):668–683, 2008.

[39] G. J. L. Naus, R. P. A. Vugts, J. Ploeg, M. J. G. van de Molengraft, and M. Steinbuch. String–stable cacc design and experimental validation: A frequency-domain approach. *IEEE Transactions on Vehicular Technology*, 59(9):4268–4279, 2010.

[40] J. Ploeg, B.T.M. Scheepers, E. van Nunen, N. Van de Wouw, and H. Nijmeijer. Design and experimental evaluation of cooperative adaptive cruise control. In *14th International IEEE Conference on Intelligent Transportation Systems*, pages 260–265, October 2011.

[41] Maarten R. I. Nieuwenhuijze, Thijs van Keulen, Sinan Oncu, Bram Bonsen, and Henk Nijmeijer. Cooperative driving with a heavy-duty truck in mixed traffic: Experimental results. *IEEE Transactions on Intelligent Transportation Systems*, 13(3):1026–1032, 2012.

[42] Road Transport Bureau, Ministry of Land, Infrastructure and Transport, Japan. `http://www.mlit.go.jp/jidosha/anzen/01asv/resourse/data/H26souchakudaisuu.pdf`. (accessed 28.03.2016, Japanese).

[43] W. J. Beaty. Traffic waves: Sometimes one driver can vastly improve traffic. `http://trafficwaves.org/`, 1998. (accessed 28.03.2016).

[44] Ryosuke Nishi, Akiyasu Tomoeda, Kenichiro Shimura, and Katsuhiro Nishinari. Theory of jam-absorption driving. *Transportation Research Part B*, 50:116–129, 2013.

[45] Katsuhiro Nishinari, Martin Treiber, and Dirk Helbing. Interpreting the wide scattering of synchronized traffic data by time gap statistics. *Physical Review E*, 68(6):067101, 2003.

[46] Matin Treiber and Dirk Helbing. Memory effects in microscopic traffic models and wide scattering in flow-density data. *Physical Review E*, 68(4):046119, 2003.

[47] Dirk Helbing, Ansgar Hennecke, Vladimir Shvetsov, and Martin Treiber. Micro-and macro-simulation of freeway traffic. *Mathematical and computer modelling*, 35(5):517–547, 2002.

[48] Dirk Helbing and Michael Schreckenberg. Cellular automata simulating experimental properties of traffic flow. *Phys. Rev. E*, 59:R2505–R2508, Mar 1999.

[49] Dirk Helbing and Mehdi Moussaid. Analytical calculation of critical perturbation amplitudes and critical densities by non-linear stability analysis of a simple traffic flow model. *The European Physical Journal B*, 69(4):571–581, 2009.

[50] Martin Treiber, Ansgar Hennecke, and Dirk Helbing. Congested traffic states in empirical observations and microscopic simulations. *Phys. Rev. E*, 62:1805–1824, Aug 2000.

[51] Martin Treiber and Arne Kesting. Traffic flow dynamics. *Traffic Flow Dynamics: Data, Models and Simulation, Springer-Verlag Berlin Heidelberg*, 2013.

[52] Boris S Kerner and H Rehborn. Experimental features and characteristics of traffic

jams. *Physical Review E*, 53(2):R1297, 1996.

[53] Joseph Treiterer. Investigation of traffic dynamics by aerial photogrammetry techniques. Technical report, 1975.

[54] Browand Fred, McArthur John, and Radovich Charles. Fuel saving achieved in the field test of two tandem trucks. *Research Reports, California Partners for Advanced Transit and Highways (PATH), Institute of Transportation Studies (UCB), UC Berkeley*, 2004.

[55] A. A. Alam, A. Gattami, and K. H. Johansson. An experimental study on the fuel reduction potential of heavy duty vehicle platooning. In *13th International IEEE Conference on Intelligent Transportation Systems*, pages 226–249, Berkeley, CA, September 2010. IEEE.

[56] Boris S. Kerner. Complexity of spatiotemporal traffic phenomena in flow of identical drivers: Explanation based on fundamental hypothesis of three-phase theory. *Phys. Rev. E*, 85:036110, Mar 2012.

[57] WenLong Jin and Wilfred W. Recker. Instantaneous information propagation in a traffic stream through inter-vehicle communication. *Transportation Research Part B*, 40(3):230 – 250, 2006.

[58] Martin Schönhof, Martin Treiber, Arne Kesting, and Dirk Helbing. Autonomous detection and anticipation of jam fronts from messages propagated by intervehicle communication. *Transportation Research Record*, 1999(1):3–12, 2007.

[59] Bart Netten, Andreas Hegyi, Meng Wang, WJ Schakel, Yufei Yuan, Thomas Schreiter, Bart Van Arem, Coen Van Leeuwen, and Tom Alkim. Improving moving jam detection performance with v2i communication. In *Proceedings of the 20th ITS world congress on intelligent transport systems, TS102, Tokyo, Japan, Oct. 14-18, 2013. Best Paper Award Scientific Paper. Authors version.* ITS Japan, 2013.

Appendix A

Appendix from Theory of JAD

A.1 Derivation of the stability of Helly model

In the case of Helly model, from the result of C Liang and H Peng [26], the condition of stability can be calculated, even with a reaction time delay of drivers.

Considering a platoon of vehicles with the same velocity and the same inter-vehicular distance, each vehicle in this string can be modeled as following:

$$\begin{aligned} x_i &= \frac{1}{s} v_i \\ v_i &= G_i(s) \cdot v_{i-1} \end{aligned} \tag{A.1}$$

where v_i is the velocity of the ith vehicle and G_i represents the car-following algorithm of the ith vehicle. For each vehicle, the following errors are defined:

$$\begin{aligned} \epsilon_i &= x_{i-1} - x_i - D_i \\ \epsilon_{vi} &= v_{i-1} - v_i \end{aligned} \tag{A.2}$$

where D_i denotes the desired range for the ith vehicle. In this paper we have assumed constant time-headway policy is adopted for all vehicles, that is, the desired ranges are proportional to vehicle speeds. Let $D_i = h_i \cdot v_i$ (h_i is the constant time-headway for the ith vehicle), then the range errors ϵ_i can be rewritten as:

$$\epsilon_i = x_{i-1} - x_i - h_i \cdot v_i \tag{A.3}$$

To investigate the string stability of such a system, a propagation transfer function $\bar{G}_i$, is defined as the transfer function from range error of ith vehicle to the range error of the $i+1$th vehicle.

$$\bar{G}_i = \frac{\epsilon_{i+1}}{\epsilon_i} \tag{A.4}$$

Substituting (A.1) and (A.2) into (A.3), we have

$$\begin{aligned}
\bar{G}_i &= \frac{\epsilon_{i+1}}{\epsilon_i} \\
&= \frac{x_i - x_{i+1} - D_{i+1}}{x_{i-1} - x_i - D_i} \\
&= \frac{\frac{1}{s}v_i - \frac{1}{s}v_{i+1} - h_{i+1} \cdot v_{i+1}}{\frac{1}{s}v_{i-1} - \frac{1}{s}v_i - h_{i+1} \cdot v_{i+1}} \\
&= \frac{\frac{1}{s}v_i - \frac{1}{s} \cdot G_{i+1}(s) \cdot v_i - h_{i+1} \cdot G_{i+1}(s) \cdot v_i}{\frac{1}{s} \cdot \frac{1}{G_i(s)} \cdot v_i - \frac{1}{s}v_i - h_i \cdot v_i} \\
&= \frac{1 - G_{i+1}(s) - s \cdot h_{i+1} \cdot G_{i+1}(s)}{\frac{1}{G_i(s)} - 1 - s \cdot h_i}
\end{aligned} \tag{A.5}$$

if $G_{i+1} = G_i$ and $h_{i+1} = h_i$ i.e. the consecutive ith and $i+1$th vehicle is the same policy of determining the vehicle's velocity, the transfer function $\bar{G}_i$ is mentioned bellow

$$\bar{G}_i = G_i = G. \tag{A.6}$$

As the case of Helly model, the formula of Helly model is written as following statement

$$\dot{v_i} + \tau\ddot{v_i} = k_1(x_{i-1} - x_i - T_m v_i - d) + k_2(v_{i-1} - v_i), \tag{A.7}$$

where we assume T_m is the time-headway and the value is constant. Giving Laplace transform into (A.7), the formula is changed into

$$
\begin{aligned}
sv_i + s^2\tau v_i &= k_1(\frac{1}{s}v_{i-1} + \frac{x_{i-1}(0)}{s} - \frac{1}{s}v_i - \frac{x_i(0)}{s} - T_m \cdot v_i - \frac{d}{s}) + k_2(v_{i-1} - v_i) \\
&= k_1(\frac{1}{s}v_{i-1} - \frac{1}{s}v_i - T_m v_i) + k_2(v_{i-1} - v_i). \qquad \text{(A.8)}
\end{aligned}
$$

we divide the formula (A.8) into v_i and v_{i-1}

$$
(\tau s^3 + s^2 + (k_1 T_m + k_2)s + k_1)v_i = (k_2 s + k_1)v_{i-1}. \qquad \text{(A.9)}
$$

We can obtain the system gain G as

$$
G = \frac{k_2 s + k_1}{\tau s^3 + s^2 + (k_1 T_m + k_2)s + k_1}. \qquad \text{(A.10)}
$$

if traffic system is stable, for the transfer function $\bar{G}_i = G$,

$$
\forall s = j\omega \qquad |G| \leq 1 \qquad \text{(A.11)}
$$

is needed, where j is the imaginary unit and ω is a frequency of input wave.

Substituting $s = j\omega$ into $|G|$,

$$
\begin{aligned}
|G| &= |\frac{jk_2\omega + k_1}{-j\tau\omega^3 - \omega^2 + j(k_1 T_m + k_2)\omega + k_1}| \\
&= \frac{|jk_2\omega + k_1|}{|j(-\tau\omega^3 + (k_1 T_m + k_2)\omega) - \omega^2 + k_1|} \leq 1. \qquad \text{(A.12)}
\end{aligned}
$$

Transposing left hand side to right hand side, we can obtain

$$
\begin{aligned}
|j(-\tau\omega^3 + (k_1 T_m + k_2)\omega) - \omega^2 + k_1| &\geq |jk_2\omega + k_1| \\
(\tau\omega^3 - (k_1 T_m + k_2)\omega)^2 + (\omega^2 - k_1)^2 &\geq {k_2}^2\omega^2 + {k_1}^2 \\
\tau^2\omega^6 - 2\tau(k_1 T_m + k_2)\omega^4 + (k_1 T_m + k_2)^2\omega^2 + \omega^4 - {k_2}^2\omega^2 - 2k_1\omega^2 &\geq 0 \\
\tau^2\omega^4 + (1 - 2\tau(k_1 T_m + k_2))\omega^2 + (k_1 T_m + k_2)^2 - {k_2}^2 - 2k_1 &\geq 0 \\
\tau^2 X^2 + (1 - 2\tau(k_1 T_m + k_2))X + (k_1 T_m + k_2)^2 - {k_2}^2 - 2k_1 &\geq 0, \qquad \text{(A.13)}
\end{aligned}
$$

where we are replace ω^2 into X. To satisfy (A.11) is equal with that all $X > 0$ satisfies (A.13). For that, it is good to satisfy

$$(i) \quad \text{The discriminant of existence of second degree equation } : D \leq 0 \tag{A.14}$$

or

$$(ii) \quad 1 - 2\tau(k_1 T_m + k_2) > 0 \quad \text{and} \quad (k_1 T_m + k_2)^2 - {k_2}^2 - 2k_1 \geq 0. \tag{A.15}$$

That is

$$\begin{aligned} (i) \quad D &= (1 - 2\tau(k_1 T_m + k_2))^2 - 4\tau^2((k_1 T_m + k_2)^2 - {k_2}^2 - 2k_1) \\ &= 1 - 4\tau(k_1 T_m + k_2) + 4\tau^2 {k_2}^2 + 8k_1\tau^2 \leq 0 \end{aligned}$$

$$\begin{aligned} &\Leftrightarrow k_1 T_m + k_2 \geq ({k_2}^2 + 2k_1)\tau + \frac{1}{4\tau} \\ &\Leftrightarrow T_m \geq -\frac{k_2}{k_1} + \frac{1}{4k_1\tau} + \frac{{k_2}^2}{k_1}\tau + 2\tau \end{aligned} \tag{A.16}$$

or

$$(ii) \quad T_m \leq -\frac{k_2}{k_1} + \frac{1}{2k_1\tau} \quad \text{and} \quad T_m \geq \frac{-k_2 + \sqrt{{k_2}^2 + 2k_1}}{k_1}. \tag{A.17}$$

In the case where vehicles has no reaction time delay, that is, $\tau = 0$, the inequality (A.16) is not always satisfied and the left side of the inequality (A.17) is always satisfied. Thus the the condition of the stability is

$$T_m \geq \frac{-k_2 + \sqrt{{k_2}^2 + 2k_1}}{k_1}. \tag{A.18}$$

Appendix B

Appendix from Numerical simulation of JAD

B.1 JAD for cars close to leading car

We only discuss the case $h_{\mathrm{buf}} = 1.09$ because the approach is the same for other values of h_{buf}. The dotted lines in Fig. B.1 depict the relationship between T_{a} and v_{a} required to satisfy JAD [Eq. (3.7)] from $m = 10$ to $m = 90$ in steps of 10. In addition, we depict Eq. (3.7) from $m = 100$ to large values of m in steps of 10. We use black dashed lines to show the boundary for secondary traffic jams and thick black lines to show the boundary for the restriction of the onset of JAD [given by inequality (3.8)]. As m increases from 50 to 100, each dotted line shifts to the upper region, which agrees with the positional relationship of the lines of Eq.(3.7) for $m > 100$. In contrast, each dotted line shifts to a lower region as m increases from 10 to 50. Tentatively, we attribute this nonconstant nature of m to the nonconstant dependence of Δ_m on m. When the perturbation caused by car 1 propagates to nearby cars, the perturbation does not grow to a sufficiently large magnitude. Because of the small magnitude of the perturbation, the car preceding the absorbing car (car $m-1$) is close to car 1 and does not have to increase its headway. Thus, the headway of car $m-1$ is less than the initial headway Dh_{buf} after coming out of the perturbation. Because the headway of car $m-1$ after coming out of the traffic jam is less than Dh_{buf} , Δ_{m-1} is less than Δ_{m-2}. Thus, the T_{a} line for the absorbing car m is depicted below that of the absorbing car $m-1$. In addition, the boundary for starting JAD for $m < 50$ differs from that for $m > 50$. The boundary of the restriction for each m corresponds to the intersection point that satisfies Eq. (3.7)

and $T_{\rm a} + 2\frac{v_{\rm MAX}-v_{\rm a}}{\alpha_{\rm a}} = t_{G_{m-1}} - t_{S_1}$; i.e., the boundary is affected by the characteristics of $T_{\rm a}$ [Eq. (3.7)]. Thus we guess the different boundary is caused by the nonconstant characteristic of $T_{\rm a}$.

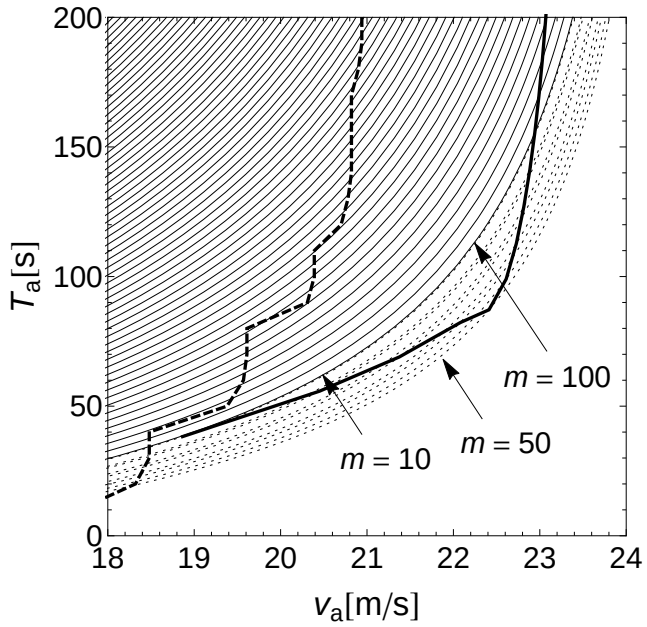

Fig. B.1. The relationships between $T_{\rm a}$ and $v_{\rm a}$ that must be satisfied for JAD [Eq. (3.7)] depicted by black dotted lines for $m = 10, 20, \ldots, 90$ and by black thin lines for $m = 100, 110, \ldots$. The boundary for the onset of secondary traffic jams is depicted by a broken black line and the line representing the JAD starting-time restriction is depicted by a thick black line. The restriction line is obtained by connecting the points of ($v_{\rm a}$, $T_{\rm a}$) that satisfy the simultaneous equations (3.7) and $T_{\rm a} + 2\frac{v_{\rm MAX}-v_{\rm a}}{\alpha_{\rm a}} = t_{G_{m-1}} - t_{S_1}$ for m from 10 to 1000 in steps of 10.

B.2 Robustness of JAD against $\alpha_{\rm a}$

We numerically investigate the robustness of JAD against a parameter of acceleration $\alpha_{\rm a}$. Figs. B.2(a) and B.2(b) display the region of successful JAD in $v_{\rm a} - T_{\rm a}$ diagrams obtained with $\alpha_{\rm a} = 0.2$ [m/s^2] and 0.8 [m/s^2], respectively. Note that we set $\alpha_{\rm p} = \alpha_{\rm a}$. The regions of successful JAD exist among all the three $\alpha_{\rm a}$ values: $\alpha_{\rm a} = 0.2$ [m/s^2] [Fig. B.2(a)], $\alpha_{\rm a} = 0.4$ [m/s^2] [Fig. 3.5(c)] and $\alpha_{\rm a} = 0.8$ [m/s^2] [Fig. B.2(b)]. Moreover, shapes of the three regions are mostly unchanged. Thus, qualitative results of JAD are not influenced significantly by the choice of $\alpha_{\rm a}$.

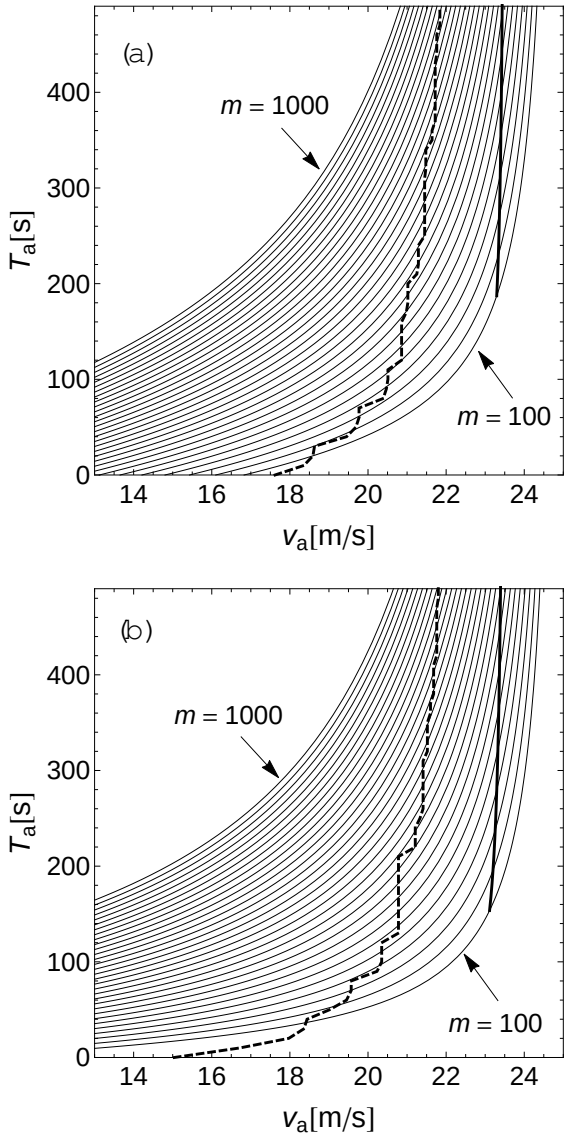

Fig. B.2. Regions of successful JAD in v_a-T_a diagrams with values of α_a other than $\alpha_a = 0.4$ [m/s^2] set in Fig. 3.5. (a) $\alpha_a = 0.2$ [m/s^2]. (b) $\alpha_a = 0.8$ [m/s^2]. We set $h_{buf} = 1.09$. Thick lines, thin lines and broken lines are depicted the same as in Fig. 3.5.

B.3 Robustness of JAD against the choice of car-following models

To show the validity of JAD in a car-following model other than the Helly model, we conduct simulations of JAD with the intelligent driver model (IDM) [50]. The definition

of IDM in our paper is the same as that in [46] as described in the following equations:

$$\dot{v_i}(t) = a\left[1 - \left(\frac{v_i(t)}{v_0}\right)^4 - \left(\frac{s^*(v_i(t), v_i(t) - v_{i-1}(t))}{x_{i-1}(t) - x_i(t) - l}\right)^2\right], \quad \text{(B.1)}$$

$$s^*(v_i(t), \Delta v_i(t)) = s_0 + v_i(t)T + \frac{v_i(t)\Delta v_i(t)}{2\sqrt{ab}}. \quad \text{(B.2)}$$

We use the same parameter values as in the original paper [46]: The desired velocity $v_0 = 120$ [km/h] $= 33.3$ [m/s], the time headway $T = 0.85$ [s], the maximum acceleration $a = 0.8$ [m/s^2], the comfortable deceleration $b = 1.8$ [m/s^2], the minimum gap $s_0 = 1.6$ [m] and the length of car $l = 6$ [m]. As in the simulations with the Helly model, each car's velocity is limited to the range $0 \leq v(t) \leq v_{\mathrm{MAX}}$, where $v_{\mathrm{MAX}} = 25$ [m/s]. In the simulation, at time $t = 0$, all the cars move at the same velocity v_{MAX} and cars 2, ..., 1000 have the same gap $(l + s_{\mathrm{e}}(v_{\mathrm{MAX}}))h_{\mathrm{buf}}$, where $s_{\mathrm{e}}(v)$ is the desired gap in a homogeneous flow with velocity v, given by [50]

$$s_e(v) = (s_0 + vT)\left(1 - \left(\frac{v}{v_0}\right)^4\right)^{-\frac{1}{2}}. \quad \text{(B.3)}$$

Other parameters such as the number of cars (1000 cars), α_{p}, T_{p} and α_{a} are the same as those in the simulation with the Helly model. The condition whereby the car-1 perturbation grows to become a jam is given by the same condition described by (3.4). It should be noted that the behavior of car 1 and the strategy of JAD that the absorbing car performs do not depend on car-following models. Fig. B.4 shows the region of successful JAD in the case of $h_{\mathrm{buf}} = 1.03$ obtained from numerical simulations. A region of successful JAD surely exists in Fig. B.4 similar to Fig. 3.5(c). Thus, JAD is robust in the two car–following models: the Helly model and IDM. We show numerically obtained trajectories of cars in time-space diagram of two patterns: (a) none of the absorbing car exists and (b) car-300 is the absorbing car and the parameter $(v_{\mathrm{a}}, T_{\mathrm{a}}) = (22.2, 246)$ in Fig.B.3(a) and (b), respectively. For (a), the perturbation caused by car-1 grows to a traffic jam. For (b), on the other hand, the absorbing car avoids being involved in the traffic jam and avoid the occurrence of the secondary jam. The boundary of the restriction of the starting time for JAD with IDM (depicted as a thick black line in Fig. B.4) goes toward smaller values of v_{a} as T_{a} increases in large values of T_{a}, compared to the boundary with the Helly model (depicted as a thick black line in Fig. 3.5 (c)). This difference between the two boundaries arises because the cars obeying IDM have a longer gap after accelerating from a small

velocity to v_{MAX} than those obeying the Helly model. The lengthened gap of each car makes the length of a jam larger. Therefore, in the numerical simulations with IDM, if the absorbing car situates in a more upstream position in the platoon, it has to perform JAD with smaller v_{a}.

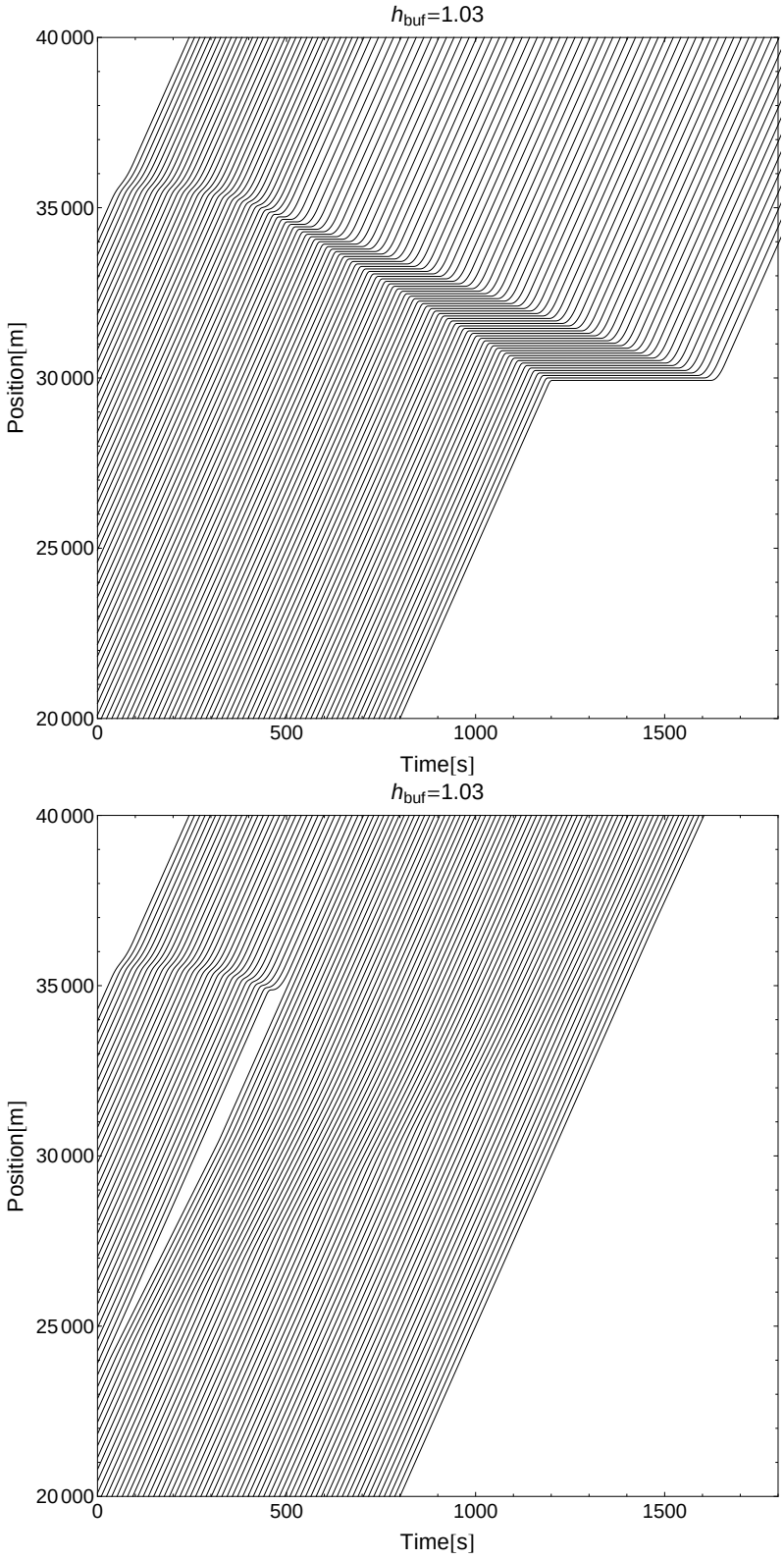

Fig. B.3. Time–space diagrams for JAD. (a) none of the absorbing car exists and (b) car-300 is the absorbing car and the parameter $(v_{\mathrm{a}}, T_{\mathrm{a}}) = (22.2, 246)$ The thick lines are trajectories of the absorbing car.

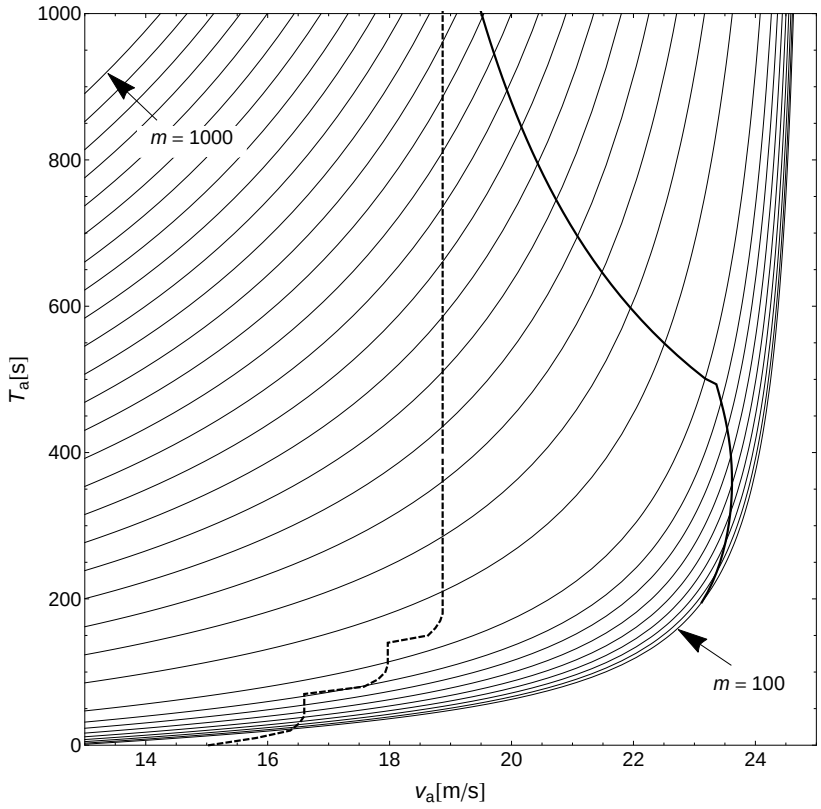

Fig. B.4. Region of successful JAD in v_{a}-T_{a} diagrams with IDM. The degree of the initial gap extension is given by $h_{\mathrm{buf}} = 1.03$. The boundary for the onset of secondary traffic jams is depicted by a broken line. The line representing the restriction of starting time for JAD is depicted by a thick line. The line of the restriction of the starting time for JAD is obtained by connecting the points of (v_{a}, T_{a}) that satisfy the simultaneous equations (3.7) and $T_{\mathrm{a}} + 2\frac{v_{\mathrm{MAX}} - v_{\mathrm{a}}}{\alpha_{\mathrm{a}}} = t_{G_{m-1}} - t_{S_1}$ for m from 100 to 1000 in steps of 10.

Appendix C

Appendix from Demonstration experiment of JAD

C.1 The boundary which distinguishes the success and failure of JAD

From chapter.4, it is found that the jam absorbing car which has middle headway (such as $h_{\mathrm{aM}} = 50$ [m]) does not avoid the traffic flow in the aspect of the travel time. In this section, we estimate the boundary of the headway which distinguishes the success and failure of JAD. Here, to estimate the boundary, we only focus the influence of the magnitude of the perturbation caused by car-1. As we mentioned in Sec.4.1.1, we assume h_i ($i = 2, \ldots, 5$) do not extend from h_0 after entangled in the perturbation. Under the assumption, in the kinematic theory in Ref. [44], the minimal distance that the absorbing car should have for JAD is determined by only the magnitude of the perturbation from car-1. In this section, we regard the perturbation as the loss of the travel distance of car-1. We denoted the loss as Δ and it is calculated by $\int_{v_{\mathrm{FM}}>v}(v_{\mathrm{FM}} - v)\mathrm{d}t$, where v_{FM} is the measured values of car-1 near the perturbation. The measuring procedure of Δ is explained in the caption of Fig. C.1. We list h_{aM} and Δ in Tab. C.1.

To calculate the boundary, we use the support vector machine (SVM) in two dimensions of h_{aM} and Δ. As the calculation technique, we use the function "svmtrain" in LIBSVM, a library for SVM, on MATLAB. We choose the parameter "cost", which is an optional parameter of svmtrain, as 1000. Other parameters are set to the initial values. With the

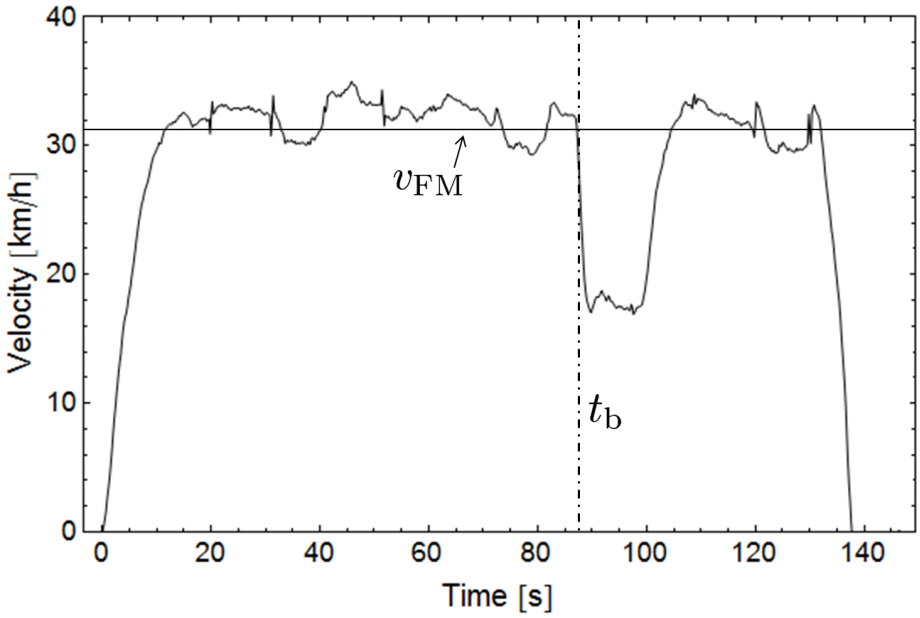

Fig. C.1. A time series velocity and v_{FM} of car-1 from trial 11. t_{b} is determined as the same way as that in Sec.4.2. v_{FM} is calculated as the mean velocity of car-1 for 20 [s] immediately before t_{b}. The magnitude of the perturbation corresponds to the region which is sandwiched by the diagram and the black horizontal line.

No.	h_{aM} [m]	Δ	success/failure
1	16.3	58.6	×
2	14.1	67.5	×
3	15.3	64.4	×
4	15.4	57.6	×
5	15.9	51.6	×
6	17.2	52.6	×
7	21.4	58.5	×
8	20.9	58.1	×
9	18.5	51.9	×
10	18.3	50.5	×
11	143.8	51.8	◯
12	120.2	61.5	◯
13	64.1	58.3	◯
14	62.6	58.3	◯
15	71.1	57.8	◯
16	56.4	52.9	◯
17	40.4	52.2	×
18	39.6	55.5	×
19	42.9	53.4	×

Table. C.1. Trial number, measured parameters h_{aM}, Δ, and success or failure of JAD. The procedure of measuring h_{aM} and Δ is described in Fig. C.1 and its caption. In each trial, absorption driving is said to succeed if v_{min} exceeds 5.56 [m/s] (=20 [km/h]), and to fail otherwise. v_{min} is shown in Tab.4.1in Sec.4.2. Success and failure of JAD are denoted by ◯ and ×, respectively.

technique, we obtain the boundary which is given by

$$h_{\mathrm{aM}} = 0.1853\Delta + 39.803. \tag{C.1}$$

Figure C.2 plots the relationship between h_{aM} and Δ for each trial, where successful and failed trials are represented by circles and cross marks, respectively, and the boundary as the solid straight line. In the situation of our experiment, Δ is from 50 to 70. Thus, the value of the headway of the absorbing car on the boundary is around 50 [m].

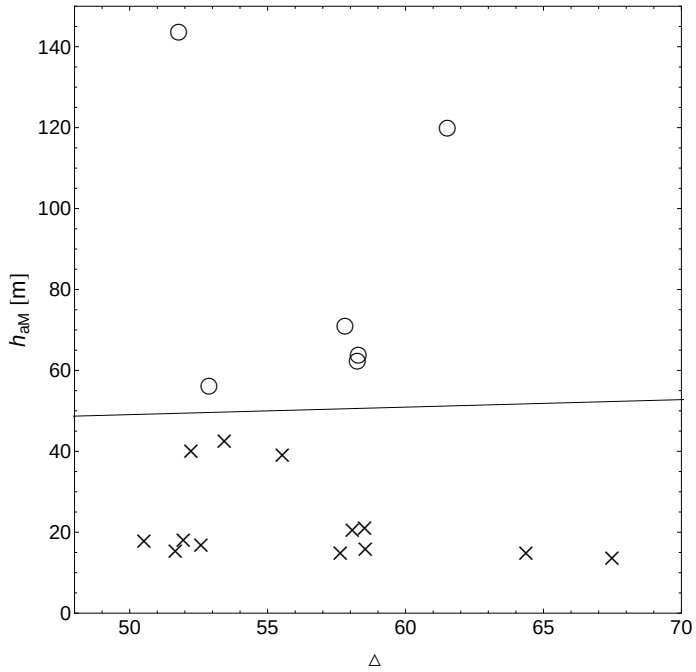

Fig. C.2. Two-dimensional diagram of h_{aM} versus Δ in the 19 trials. Circles and cross marks denote success and failure of JAD, respectively, judged by the criterion 5.56 [m/s]. The straight line in the diagram corresponds to the boundary calculated with the SVM. The slope and h_{aM}-intercepts are 0.185 and 39.8, respectively.